Landau levels in strained two-dimensional photonic crystals

J. Guglielmon, M. C. Rechtsman, and M. I. Weinstein

Phys. Rev. A **103**, 013505 — Published 5 January 2021

DOI: 10.1103/PhysRevA.103.013505

Landau levels in strained two-dimensional photonic crystals

J. Guglielmon[1] and M. C. Rechtsman[1]
[1]*Department of Physics, The Pennsylvania State University, University Park, PA 16802, USA*

M. I. Weinstein[2]
[2]*Department of Applied Physics and Applied Mathematics and Department of Mathematics, Columbia University, New York, NY, 10027 USA*

The principal use of photonic crystals is to engineer the photonic density of states, which controls light-matter coupling. We theoretically show that strained 2D photonic crystals can generate artificial electric and magnetic fields that act on light and we show that particular strain patterns give rise to highly degenerate Landau levels. Since photonic crystals are not in general described by tight-binding models, we employ a multiscale expansion of the full continuum wave equation. Using numerical simulations, we observe dispersive Landau levels which we show can be flattened by engineering a pseudoelectric field. Artificial fields yield a design principle for aperiodic nanophotonic systems.

In the presence of strain, graphene exhibits a remarkable effect: an inhomogeneous deformation of the lattice induces a strong pseudomagnetic field governing the low energy theory [1–6]. If the strain is designed to produce a uniform pseudomagnetic field, highly degenerate Landau levels form at energies near the Dirac points. In photonic systems, methods for generating pseudomagnetic fields [7–10] are of significant interest since photons are fundamentally uncharged and therefore do not directly respond to real magnetic fields. If Landau levels could be realized in the nanophotonic domain using strained photonic crystals, the associated large density of states could used to enhance light-matter interactions (e.g., the Purcell effect [11] or nonlinear phenomena [12]).

Strain-induced pseudomagnetic fields have been demonstrated experimentally in photonic systems of coupled waveguide arrays [13], exciton-polariton condensates based on coupled cavities [14, 15], and microwave systems of coupled resonators [16]. Photonic Landau levels have also been discussed in the context of lasing models [17] and strain and related ideas have been explored as a means for producing pseudomagnetism in acoustic systems [18–20]. In the waveguide arrays studied in [13], however, time is mapped to a spatial dimension, and thus energy eigenvalues do not correspond to mode frequencies but to propagation constants. Hence, the Landau levels will not directly alter the photonic density of states. Demonstrations based on coupled resonators can be treated with the standard tight-binding framework often used to study strained graphene. Photonic crystals, however, are governed by the continuum Maxwell equations to which tight-binding models do not generally apply [21].

In this Letter, we address the question: Since Dirac points generically emerge in the presence of certain symmetries, [22–24] and therefore occur also in photonic crystals, can strain be used to generate pseudomagnetic fields for light in the nanophotonic domain? To answer this question, we use a two-scale expansion of solutions to the full continuum wave equation to show that pseudomagnetic and pseudoelectric fields are present in a class of deformed 2D photonic crystals. Our results, which apply to wave equations in non-dissipative media, require only that the strain be slowly varying and that the unstrained periodic structure exhibit Dirac points associated with a certain set of symmetries. The effective equations contain no free parameters. We make no assumptions about the magnitude of the material (index) contrast and our results do not require an effective tight-binding model.

We assess the validity of our effective theory by performing full-wave numerical simulations in an experimentally realistic strained photonic crystal of air holes embedded in silicon. These simulations demonstrate high density of states at energies corresponding to the Landau levels of the effective theory. However, the Landau levels are weakly dispersive and we find that producing nearly flat (non-dispersive) Landau levels in such a photonic crystal can be achieved using a new ingredient: a strain that, on the level of the effective equations, generates a pseudoelectric field (in addition to the pseudomagnetic field), and on the level of the full wave equation, acts to flatten the bands.

We begin by considering light propagating in the plane of a two-dimensional photonic crystal: a medium consisting of a real, spatially varying scalar dielectric $\varepsilon(\mathbf{x})$ that is uniform in the x_3 direction, so that we may take $\mathbf{x} = [x_1, x_2]$. The solutions can be classified as having either TE or TM polarization. For time-harmonic solutions with electric and magnetic fields $\mathbf{E}(\mathbf{x}, t) = \mathbf{E}(\mathbf{x})e^{-i\omega t}$ and $\mathbf{H}(\mathbf{x}, t) = \mathbf{H}(\mathbf{x})e^{-i\omega t}$, the modes are governed by the scalar Helmholtz equation

$$-\nabla \cdot \big(\xi(\mathbf{x})\nabla\big)\psi(\mathbf{x}) = (\omega/c)^2\rho(\mathbf{x})\psi(\mathbf{x}), \qquad (1)$$

where c denotes the vacuum speed of light. For TE polarization, $\xi(\mathbf{x}) = 1/\varepsilon(\mathbf{x})$, $\rho(\mathbf{x}) = 1$, and the scalar function $\psi(\mathbf{x})$ gives the magnetic field $\mathbf{H}(\mathbf{x}) = \psi(\mathbf{x})\hat{\mathbf{z}}$. For TM polarization, $\xi(\mathbf{x}) = 1$, $\rho(\mathbf{x}) = \varepsilon(\mathbf{x})$, and $\psi(\mathbf{x})$ gives the electric field $\mathbf{E}(\mathbf{x}) = \psi(\mathbf{x})\hat{\mathbf{z}}$.

To obtain a structure possessing Dirac points, we require that $\varepsilon(\mathbf{x})$ is inversion symmetric, C_3 rotation invariant, and translation invariant with respect to the

triangular lattice $\mathbb{Z}\mathbf{R}_1 \oplus \mathbb{Z}\mathbf{R}_2$, where $\mathbf{R}_1 = a[1,0]$ and $\mathbf{R}_2 = a[1/2, \sqrt{3}/2]$ and a denotes the lattice constant. It was proved in [22–24] for continuum media that these conditions imply the existence of Dirac points at the Brillouin zone vertices $\mathbf{K} = (\mathbf{G}_1 - \mathbf{G}_2)/3$, $\mathbf{K}' = -\mathbf{K}$, where $\mathbf{G}_1$ and $\mathbf{G}_2$ are the reciprocal lattice vectors. For a Dirac point occurring at quasimomentum $\mathbf{k}_D$ and energy E_D, two consecutive bands $E_\pm(\mathbf{k})$ of the operator defined in Eq. (1) (with $E = \omega^2/c^2$) exhibit a conical intersection

$$E_\pm(\mathbf{k}) \;=\; E_D \;\pm\; \mathrm{v}_D\,|\mathbf{k}-\mathbf{k}_D|\;(1+\mathcal{O}(|\mathbf{k}-\mathbf{k}_D|) \qquad (2)$$

for $\mathbf{k}$ near $\mathbf{k}_D$.

Since $\omega^2 = c^2 E$ there are positive and negative branches of frequencies, ω, obtained from (2). We focus on the positive branch, yielding

$$\omega_\pm(\mathbf{k}) = \omega_D \pm (\mathrm{v}_D c^2/(2\omega_D))\;|\mathbf{k}-\mathbf{k}_D|\;(1+\mathcal{O}(|\mathbf{k}-\mathbf{k}_D|)\,. \qquad (3)$$

We now focus on the Dirac point at $\mathbf{k}_D = \mathbf{K}$; the case $\mathbf{k}_D = \mathbf{K}' = -\mathbf{K}$ can be treated similarly (with a pseudomagnetic field that points in the opposite direction; see the Appendix). We denote the two energy-degenerate states at the Dirac point by $\Phi_1(\mathbf{x}), \Phi_2(\mathbf{x})$. These can be taken to satisfy $\Phi_2(\mathbf{x}) = \overline{\Phi_1(-\mathbf{x})}$, $\mathcal{R}[\Phi_1] = e^{2\pi i/3}\Phi_1$, and $\mathcal{R}[\Phi_2] = e^{-2\pi i/3}\Phi_2$, where $\mathcal{R}[f](\mathbf{x}) = f(R^\dagger\mathbf{x})$ and R is a 2×2 matrix of rotation by $2\pi/3$. We use a normalization $\langle\Phi_i|\Phi_j\rangle_\rho = \delta_{ij}$. See the Appendix for more details and definitions of the two inner products $\langle f|g\rangle$ and $\langle f|g\rangle_\rho$ used in the text.

There are two parameters in the effective theory, which are computed from the eigenmodes, $\Phi_i(\mathbf{x})$, of the unstrained system, and which determine the behavior of the strained system:

$$\mathrm{v}_D = \left\langle \Phi_1 \middle| \left\{\hat{p}_1, \hat{\xi}\right\} \middle| \Phi_2 \right\rangle \qquad (4)$$

$$b_\star = \left\langle \Phi_1 \middle| \hat{p}_1 \hat{\xi}\, \hat{p}_1 \middle| \Phi_2 \right\rangle\,. \qquad (5)$$

The Dirac velocity, v_D, is associated with the slope of the dispersion relation at the Dirac point of the periodic structure [after including the factor of $c^2/(2\omega_D)$—see Eq. (3)] and $b_\star$ emerges in connection with the induced pseudomagnetic field: the ratio $b_\star/\mathrm{v}_D$ determines how strong the pseudomagnetic field will be for a given amount of strain; see Eqs. (7) and (8) below. The derivation that leads to these parameters is contained in the Appendix. Here, $\hat{p}_1 = -i\partial_{x_1}$, $\left\{\hat{p}_1, \hat{\xi}\right\} = \hat{p}_1\hat{\xi} + \hat{\xi}\,\hat{p}_1$, and $\hat{\xi}$ is the operator that acts in position space via multiplication by $\xi(\mathbf{x})$. In the Appendix, we show that both v_D and $b_\star$ can be made to be real and positive by an appropriate choice of a coordinate system and a phase convention for the eigenstates. We assume these choices have been made.

We will now consider a class of dielectric functions obtained by straining the dielectric $\varepsilon(\mathbf{x})$. We note that, while we will use the terminology of 'strain' throughout this work, we do not intend for this to be understood in the sense of a physical mechanical strain applied to a dielectric, but rather as a mathematical prescription for how one constructs the dielectric function

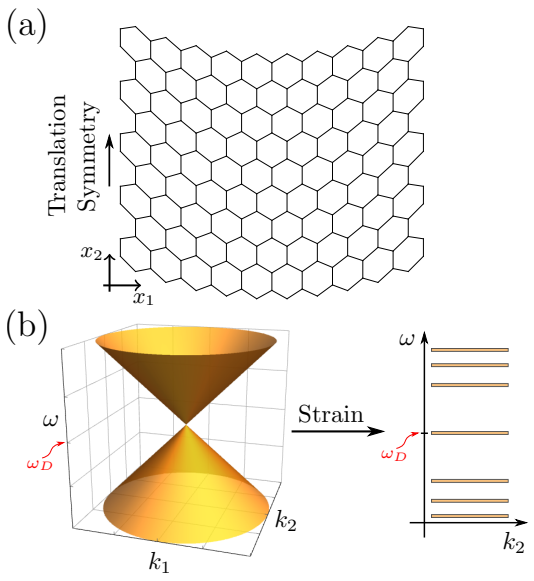

FIG. 1. (a) Illustration of a strain that produces a Landau gauge vector potential for a uniform pseudomagnetic field. (b) Schematic illustration of the effect of the strain on the spectrum. In a neighborhood of ω_D, the Dirac cone is transformed into a sequence of discrete Landau levels.

$\varepsilon'(\mathbf{x})$. Once this function has been specified, the dielectric $\varepsilon'(x)$ can be directly realized without the application of a mechanical strain (e.g., by directly etching the strained pattern into silicon, for example). A strained dielectric $\varepsilon'(\mathbf{x})$ is obtained by displacing each point $\mathbf{x}$ of the original dielectric to a new location $T(\mathbf{x}) = \mathbf{x} + \mathbf{u}(\mathbf{x})$ giving $\varepsilon'(\mathbf{x}+\mathbf{u}(\mathbf{x})) = \varepsilon(\mathbf{x})$, where $\mathbf{u}(\mathbf{x}) = (u_1(\mathbf{x}), u_2(\mathbf{x}))$. The corresponding strain matrix is denoted $U(\mathbf{x}) = \frac{1}{2}\left(D_\mathbf{x}\mathbf{u} + (D_\mathbf{x}\mathbf{u})^\top\right)$ with entries $U_{ij} = \frac{1}{2}\left(\frac{\partial u_i}{\partial x_j} + \frac{\partial u_j}{\partial x_i}\right)$ (here $[D_\mathbf{x}\mathbf{u}]_{ij} = \partial u_i/\partial x_j$). We assume that $\mathbf{u}(\mathbf{x})$ is deformed on a scale which is large compared with the lattice constant in the sense that $\mathbf{u}(\mathbf{x}) = \mathbf{f}(\kappa\mathbf{x})$, where κ is a small parameter, with units length^{-1}, that measures the length scale over which the deformation varies. Hence, $U(\mathbf{x}) \sim \mathcal{O}(\kappa)$ and one can think of κ as measuring the strain strength.

Using a general systematic perturbation theory in the small parameter κ (see the Appendix), we show that the strained dielectric $\varepsilon'(\mathbf{x})$ has modes with a two-scale spatial structure in which a pair of slowly varying amplitude functions α_i, with $i = 1$ or 2, modulate the Dirac point eigenmodes:

$$\psi(\mathbf{x}) = \sum_{i=1}^{2} \alpha_i\left(T^{-1}(\mathbf{x})\right)\Phi_i(T^{-1}(\mathbf{x})) + \mathcal{O}(\kappa). \qquad (6)$$

[As before, slowly varying is understood to mean $\alpha_i(\mathbf{x}) = g_i(\kappa\mathbf{x})$]. These modes have associated perturbed frequencies $\omega = \omega_D + \frac{c^2}{2\omega_D}E_1 + \mathcal{O}(\kappa^2)$. The amplitude functions $\alpha_i(\mathbf{x})$ and frequency perturbation E_1 (of order κ) are determined by an eigenvalue problem $\mathcal{H}_{\mathrm{eff}}\alpha'(\mathbf{x}) =$

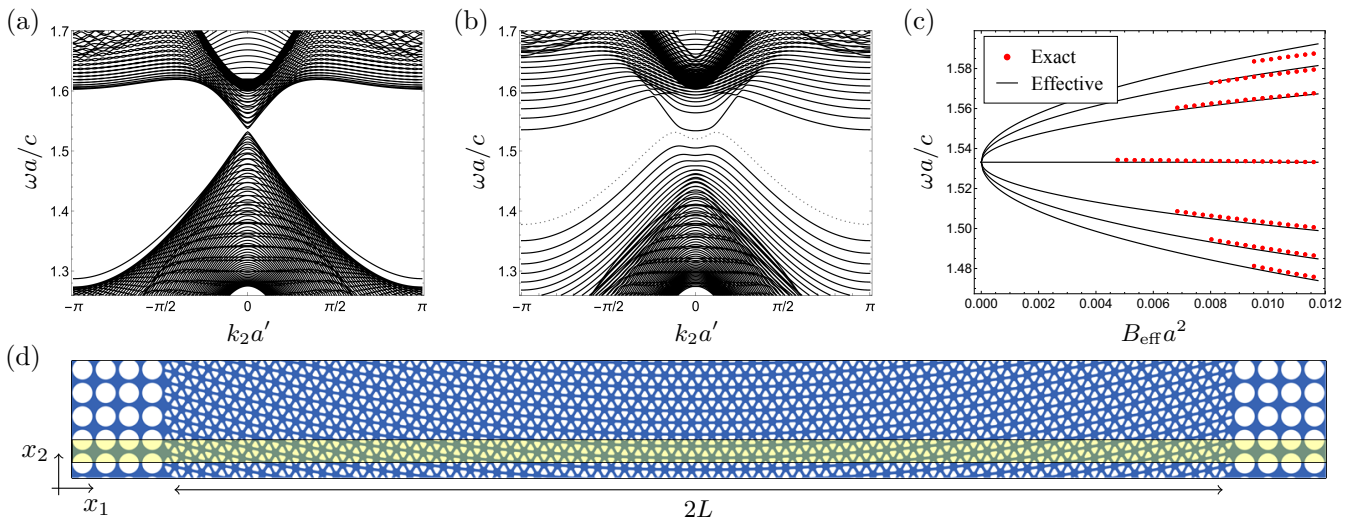

FIG. 2. (a) Full-wave band structure for TE polarized modes, showing the Dirac point of the unstrained honeycomb structure. (b) Band structure in the presence of strain, showing the emergence of Landau levels. The dashed curve corresponds a spurious mode supported at the computational boundary. (c) Level spacing as a function of the pseudomagnetic field strength. Solid curves show the prediction of Eq. (7). Red points show the spacings obtained numerically from the (full-wave) band structures at $k_2 = 0$. (d) The strained dielectric used to generate panel (b), with air holes shown in white, silicon shown in blue, and the unit cell highlighted in yellow. The strained structure is periodic under translation by a distance of $a' = \sqrt{3}a$ along the x_2 direction.

$E_1 \alpha'(\mathbf{x})$, where $\alpha'(\mathbf{x}) = [\alpha_2(\mathbf{x}),\ \alpha_1(\mathbf{x})]^T$ and $\mathcal{H}_{\rm eff}$ is a 2D Dirac Hamiltonian:

$$\mathcal{H}_{\rm eff} = \mathrm{v}_D[-i\nabla_{\mathbf{x}} - \mathbf{A}_{\rm eff}(\mathbf{x})] \cdot \sigma + W_{\rm eff}(\mathbf{x})\ \sigma_0\ , \qquad (7)$$

where $\sigma = (\sigma_1, \sigma_2)$ with σ_j denoting the Pauli matrices. The effective magnetic vector potential $\mathbf{A}_{\rm eff}(\mathbf{x})$ and electric potential $W_{\rm eff}(\mathbf{x})$ are given by

$$\mathbf{A}_{\rm eff}(\mathbf{x}) = \left(\frac{2b_\star}{\mathrm{v}_D}\right)\begin{bmatrix} +\mathrm{tr}\big(U(\mathbf{x})\sigma_3\big) \\ -\mathrm{tr}\big(U(\mathbf{x})\sigma_1\big)\end{bmatrix} \qquad (8)$$

$$W_{\rm eff}(\mathbf{x}) = -\left(\frac{\omega_D}{c}\right)^2 \mathrm{tr}\big(U(\mathbf{x})\sigma_0\big) = -\left(\frac{\omega_D}{c}\right)^2\ \nabla\cdot\mathbf{u}(\mathbf{x}). \qquad (9)$$

We emphasize that $\mathcal{H}_{\rm eff}$, $\mathbf{A}_{\rm eff}$ and $W_{\rm eff}$ emerge from a first principles derivation and depend on v_D and $b_\star$ which are completely determined by the degenerate Dirac point eigenmodes of the unstrained structure; see (4)–(5). In the Appendix, we show that the above quantities transform as expected under rotations.

We now focus on the case in which the strain produces a constant pseudomagnetic field perpendicular to the plane of the structure. As a concrete example, we consider a honeycomb lattice of air holes ($\varepsilon = 1$) embedded in silicon ($\varepsilon = 12.11$) operating in TE polarization. We take the air holes to have a triangular shape as in [25] to ensure that the frequency ω_D is not crossed by the same or other bands, *i.e.* the structure is semi-metallic at energy $(\omega_D/c)^2$; see [26, 27]. To improve numerical convergence, we take the corners of the triangles to be rounded. We take the triangle radius (center to corner) to be $r = 0.27a$ with a rounded corner radius of $r_c = 0.1a$.

We numerically compute the modes of this structure using a plane wave eigensolver (MPB) [28]. The system has a Dirac point at $\omega_D = 1.533ca^{-1}$, where the first and second TE bands touch. The quantities in Eqs. (4) and (5) are given by $\mathrm{v}_D = 0.684a^{-1}$and $b_\star = 0.502a^{-2}$. We apply a strain generated by $\mathbf{u}(\mathbf{x}) = a[0, (\kappa x_1)^2]$, where κ determines the strength of the strain. This deformation is illustrated schematically in Fig. 1(a). Note that while the strain breaks translation symmetry in the x_1 direction, the structure remains symmetric under translation by a distance $a' = \sqrt{3}a$ along the x_2 direction. From Eq. (8), the vector potential is $\mathbf{A}_{\rm eff}(\mathbf{x}) = -(4a\kappa b_\star/\mathrm{v}_D)[0, \kappa x_1]$, which is a Landau gauge vector potential for a constant effective magnetic field $\mathbf{B}_{\rm eff} = \nabla \times \mathbf{A}_{\rm eff} = -\kappa^2\ B_0 \hat{\mathbf{z}}$ with $B_0 = 4ab_\star/\mathrm{v}_D$. Since $\nabla \cdot \mathbf{u} = 0$, the strain-induced pseudoelectric potential vanishes: $W_{\rm eff}(\mathbf{x}) = 0$.

For a constant pseudomagnetic field and zero pseudoelectric potential, the eigenvalues of the Hamiltonian (7) are well-known to form a series of Landau levels consisting of discrete eigenvalues, E_1, of infinite multiplicity implying eigenvalues, ω, of the Helmholtz equation (1):

$$\omega\ =\ \omega_D \pm \frac{\mathrm{v}_D c^2}{\sqrt{2}\omega_D}\sqrt{n|\mathbf{B}_{\rm eff}(\kappa)|} + \mathcal{O}(\kappa^2),\quad n = 0, 1, 2, \ldots, \qquad (10)$$

where $|\mathbf{B}_{\rm eff}(\kappa)| = B_0\ \kappa^2$; see the Appendix.

We compare this prediction to full numerical simulations by directly solving Eq. (1) for the eigenmodes of the strained structure, again using a numerical plane wave eigensolver. We impose Bloch boundary conditions in the x_2 direction and effectively apply exponentially decaying

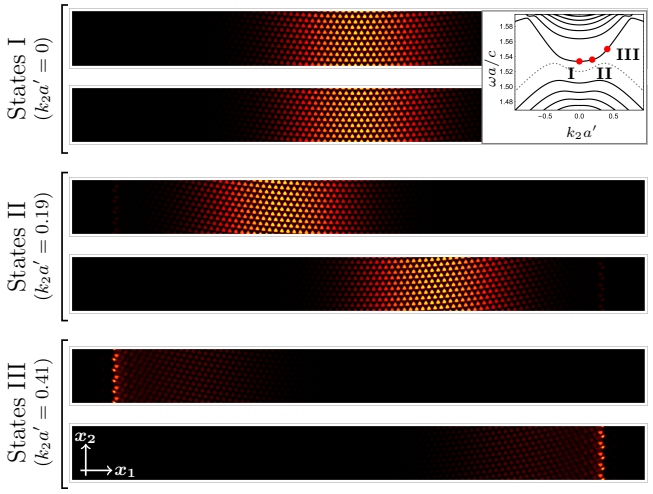

FIG. 3. Numerically computed 0-th Landau level eigenstates for the band structure of Fig. 2(b). Eigenstates correspond to the values of k_2 (I, II, and III) shown in the zoomed inset. The modes come in two-fold degenerate pairs and are localized along the x_1 direction, with centers that shift horizontally (left and right) as k_2 is varied. For large enough k_2, the states collide with the boundary and become edge states (see III).

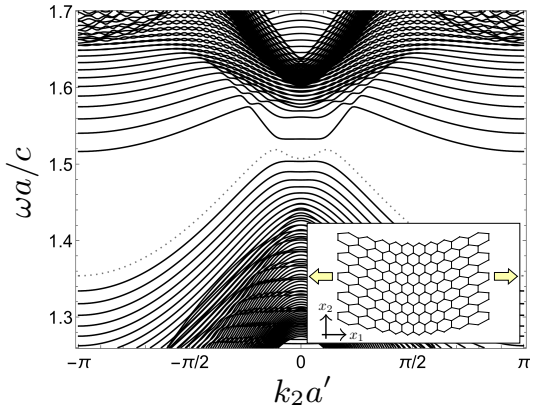

FIG. 4. Band structure obtained by beginning with the strained structure associated with Fig. 2(b) and applying an additional strain along the x_1 direction to flatten the Landau levels. Inset schematically illustrates the additional strain.

boundary conditions in the non-periodic x_1 direction by padding the boundaries with a structure that exhibits a TE band gap for $\omega \approx \omega_D$. Since the strain preserves translation symmetry along x_2, the Bloch momentum k_2 remains a good momentum. Since the supercell used for this strain pattern is invariant under translations by $\sqrt{3}a$ (as opposed to a) along x_2, both Dirac points (from $\mathbf{K}$ and $\mathbf{K}'$) reside at $k_2 = 0$. The system size along the non-periodic direction is $L = 39a$ [see Fig. 2(d)].

The numerically computed band structures are shown in Fig. 2. Upon applying the strain, the Dirac point of Fig. 2(a) splits into a sequence of discrete Landau levels shown in Fig. 2(b), which was obtained using $\kappa = 0.0548a^{-1}$. In Fig. 2(c), we compare, as a function of strain strength, the level spacings predicted by Eq. (10) to the numerically computed level spacings obtained from the band structures at $k_2 = 0$, with the results showing good agreement. Our multiscale analysis, which approximates states by spectral components near the Dirac point, is valid for $|k_2| \leq C\kappa$, for some constant C and all $\kappa a \ll 1$. As the strain is reduced, the Landau level eigenstates become progressively more delocalized along the x_1 direction and eventually reach the boundary of the computational domain. Hence, the series of simulation points in Fig. 2(c) is terminated at weak strain.

In Fig. 3, we show representative numerically obtained eigenstates. The Landau level eigenstates are localized in the x_1 direction, and are centered on a value of x_1 that varies with k_2. The eigenstates that arise from the two unique Dirac points of the unstrained structure are displaced in opposite directions as a function of k_2 (See Fig. 3 and Supplementary Materials for more information).

We note that, in general, at large x_1, the strain pattern used to generate a uniform pseudomagnetic field can become strong enough to cause the effective theory to break down in those regions. The use of a finite-width system allows one to avoid these regions. Our asymptotic analysis and full-wave numerical simulations indicate that our effective theory is valid for modes which arise from Landau levels of the effective model which are well-localized within the finite structure.

As shown in Fig. 3, at large enough k_2, the Landau level mode collides with the system boundary, causing it to become localized on the edge and rise up in frequency, giving it a non-zero group velocity. This is analogous to the way chiral edge states result from Landau levels for a system with a true magnetic field. However, in this case, the system is time-reversal symmetric (exhibiting pseudomagnetic fields that point in opposite directions at the $\mathbf{K}$ and $\mathbf{K}'$ valleys), so that both forward and backward propagating edge states exist on each edge and can scatter into one another.

Although the effective theory predicts flat Landau levels, the levels in Fig. 2(b) are weakly dispersive. This dispersion arises from contributions of order κ^2 which are neglected from the effective theory. In the Appendix, we motivate the use of a deformation of the form $\mathbf{u}(\mathbf{x}) = a[\beta(\kappa x_1)^3, (\kappa x_1)^2]$ for mitigating this dispersion. On the level of the effective equations, this yields $\mathbf{B}(\mathbf{x}) = -(4a\kappa^2 b_\star/\mathrm{v}_D)\hat{\mathbf{z}}$ as before, but now with a quadratic potential $W_{\mathrm{eff}}(\mathbf{x}) = 3a\beta\kappa(\omega_D/c)^2(\kappa x_1)^2$, corresponding to a pseudoelectric (as opposed to pseudomagnetic) field, which can be used as a tool to compensate for the dispersion. Note that this is not required in the graphene picture of pseudomagnetism [2]. It is required in the continuum photonic crystal setting because of a lack of an accurate nearest-neighbor tight-binding model. The numerically computed band structures that result from taking $\kappa = 0.0548a^{-1}$ and $\beta = 0.0380$ are shown in Fig. 4, where we see a clear flattening of the

Landau levels.

In conclusion, we have shown that, for a class of 2D photonic crystals possessing Dirac points, strain produces pseudoelectric and pseudomagnetic fields for photons. Explicit expressions for all parameters of the effective Hamiltonian are given in terms of the Bloch eigenmodes at the Dirac point of the unstrained structure. There are no free parameters. The modes of the strained structure are constructed as slow modulations of deformed Dirac point eigenmodes. The modulations are governed by a Dirac equation with effective magnetic and electric potentials. Using a specific strain pattern, we have demonstrated the emergence of Landau levels in a photonic crystal that could be realized using standard fabrication techniques in silicon photonics. We found that a conventional strain (as in graphene) gives rise to dispersive Landau levels, but that dispersion can be corrected for (i.e., the bands can be flattened) using a strain that induces an additional pseudoelectric field that does not alter the original pseudomagnetic field. As with other flat band systems, an important challenge relevant to the experimental realization of our structure will be the issue of increased sensitivity to disorder, an issue that is well-known to occur for slow-light and flat band systems [29].

Multiscale analysis enables treatment of dielectric structures that cannot be treated with band theory. This technique could be applied to general aperiodic media that arise as slowly varying deformations of periodic media, including media not amenable to tight-binding methods. This approach provides an analytical handle on and physical intuition for such systems that, in many settings, require prohibitive numerical simulations. We envision that strain-induced pseudomagnetic and pseudoelectric fields will be useful for applications, particularly in the nanophotonic domain, such as chip-scale nonlinear optics and coupling to quantum emitters, where the high density-of-states associated with flat bands implies strong enhancement of light-matter interaction.

ACKNOWLEDGMENTS

M.C.R. and J.G. acknowledge the support of the National Science Foundation under award number DMS-1620422, the ONR YIP program under grant number N00014-18-1-2595, as well as the Packard Foundation under fellowship number 2017-66821. M.I.W was supported in part by DMS-1412560, DMS-1620418, DMS-1908657 and Simons Foundation Math + X Investigator Award #376319. He acknowledges stimulating discussions with A. Drouot and J. Shapiro.

Appendix A: Media with Dirac points

1. Overview and the relevant wave equations

In the following appendices, we give a detailed derivation of the results presented in the main text. Starting with a general class of continuum partial differential equations, which includes the single particle Schrödinger equation and the Maxwell equations for 2D photonic crystals (we treat both TE and TM polarization), we apply a multiple scale perturbation analysis to non-uniformly deformed honeycomb structures to derive the effective equations governing wave packets that are constructed from states with energies near E_D (the energy of the Dirac point in the undeformed structure). The resulting effective Hamiltonian is a Dirac Hamiltonian with an *effective magnetic potential* and an *effective electric potential*, both generated by the prescribed deformation. We derive expressions for all parameters of the effective theory in terms of the bulk modes of the unstrained structure. The theory contains no free parameters. Our arguments work for arbitrary finite contrast and no tight-binding regime is required. The analysis can be adapted to other wave equations, *e.g.* acoustics, elasticity. We also provide details relating to the particular deformations discussed in the main text, which are designed to generate a flat Landau level spectrum.

We consider wave equations which arise in quantum and classical physics:

The *Schrödinger equation*

$$i\partial_t \Psi \;=\; H\Psi \;=\; \left(-\Delta + V(\mathbf{x})\right)\Psi \tag{A1}$$

and the *classical wave equation*

$$c^{-2}\;\rho(\mathbf{x})\;\partial_t^2 \Psi \;-\nabla_{\mathbf{x}}\cdot\xi(\mathbf{x})\nabla_{\mathbf{x}}\Psi \;=\; 0. \tag{A2}$$

In the above equations, $V(\mathbf{x})$ is real-valued, $\rho(\mathbf{x})$ is real-valued and strictly positive, and $\xi(\mathbf{x})$ is a symmetric 2×2 matrix whose eigenvalues are bounded away from zero, uniformly in $\mathbf{x}$. For simplicity, $\xi(\mathbf{x})$, $\rho(\mathbf{x})$ and $V(\mathbf{x})$ are taken to be smooth in $\mathbf{x}$.

Time-harmonic solutions, $\Psi(\mathbf{x},t) = e^{-i\omega t}\psi(\mathbf{x})$, are determined by the solutions of the Helmholtz / Schrödinger spectral problem:

$$\left(\;-\nabla_{\mathbf{x}}\cdot\xi(\mathbf{x})\nabla_{\mathbf{x}} \;+\; V(\mathbf{x})\;\right)\psi \;=\; E\;\rho(\mathbf{x})\psi \tag{A3}$$

where we have combined the Schrödinger and classical cases to facilitate a unified treatment of Eqs. (A1) and (A2). In particular, the time-independent equation (A3) incorporates several cases of interest:

(1) Schrödinger: $\xi(\mathbf{x}) = I_{2\times 2}$, $\rho(\mathbf{x}) \equiv 1$, $V(\mathbf{x})$ = potential

(2) Maxwell TM: $\xi(\mathbf{x}) = I_{2\times 2}$, $\rho(\mathbf{x}) = \varepsilon(\mathbf{x})$, $V(\mathbf{x}) = 0$, $E = (\omega/c)^2$

(3) Maxwell TE: $\xi(\mathbf{x}) = [\varepsilon(\mathbf{x})]^{-1}$, $\rho(\mathbf{x}) = 1$, $V(\mathbf{x}) = 0$, $E = (\omega/c)^2$.

We may write (A3) as

$$\mathcal{L}_{\xi,\rho}\ \psi \ = \ E\ \psi$$
$$\mathcal{L}_{\xi,\rho} \ = \ \frac{1}{\rho(\mathbf{x})}\ \Big(-\nabla_{\mathbf{x}} \cdot \xi(\mathbf{x}) \nabla_{\mathbf{x}} \ + \ V(\mathbf{x})\ \Big). \qquad \text{(A4)}$$

Consider the case where $\xi(\mathbf{x}), \rho(\mathbf{x})$ and $V(\mathbf{x})$ are periodic with respect to a lattice, $\Lambda = \mathbb{Z}\mathbf{v}_1 \oplus \mathbb{Z}\mathbf{v}_2 \subset \mathbb{R}^2_{\mathbf{x}}$, where $\mathbf{v}_i$ are the lattice vectors. We denote a choice of unit cell by Ω, the dual lattice by Λ^*, and a dual unit cell in $\mathbb{R}^2_{\mathbf{k}}$ by $\mathcal{B}$ (Brillouin zone). $\mathcal{L}_{\xi,\rho}$ is self-adjoint with respect to the inner product[1]

$$\langle f, g \rangle_\rho \ = \ \int_\Omega \ \overline{f(\mathbf{x})} g(\mathbf{x})\ \rho(\mathbf{x})\ d\mathbf{x}.$$

and has a (Bloch) band spectrum. We denote its bands by:

$$E_1(\mathbf{k}) \leq E_2(\mathbf{k}) \leq \cdots \leq E_b(\mathbf{k}) \leq \ldots, \quad \mathbf{k} = (k_1, k_2) \in \mathcal{B}.$$

Remark A.1 *For Maxwell's equations ($V = 0$), $\mathcal{L}_{\xi,\rho}$ is a non-negative self-adjoint operator and hence $E_b(\mathbf{k}) \geq 0$ for all $b \geq 1$. Since $(\omega/c)^2 = E$, there are two families of bands given by: $\omega_{b,\pm}(\mathbf{k}) \ = \ \pm c\sqrt{E_b(\mathbf{k})}$. For simplicity, we focus on the positive branch.*

2. Bulk honeycomb media

Assume now that Λ denotes the equilateral triangular lattice in $\mathbb{R}^2$. For each $\mathbf{v} \in \Lambda$ let $T_{\mathbf{v}}[f](\mathbf{x}) = f(\mathbf{x}+\mathbf{v})$. We say that $\mathcal{L}_{\xi,\rho}$, defined in (A4), models a *bulk honeycomb medium* if:

$$[T_{\mathbf{v}}, \mathcal{L}_{\xi,\rho}] = 0, \quad \text{for all } \mathbf{v} \in \Lambda$$
$$[\mathcal{C}, \mathcal{L}_{\xi,\rho}] = 0, \quad [\mathcal{P}, \mathcal{L}_{\xi,\rho}] = 0, \quad [\mathcal{R}, \mathcal{L}_{\xi,\rho}] = 0.$$

Here, $\mathcal{C}[f](\mathbf{x}) = \overline{f(\mathbf{x})}$, $\mathcal{P}[f](\mathbf{x}) = f(-\mathbf{x})$ and $\mathcal{R}[f](\mathbf{x}) = f(R^*\mathbf{x})$, where R is a 2×2 matrix of rotation by $2\pi/3$. That is, the coefficients of $\mathcal{L}_{\xi,\rho}$ are $\Lambda-$ periodic, real-valued and, with respect to some origin of coordinates (taken to be $\mathbf{x}_0 = 0$) inversion-symmetric and $2\pi/3-$ rotationally invariant. With regard to $\xi(\mathbf{x})$, we focus on the isotropic case:

$$\xi = \xi(\mathbf{x})\ I_{2\times 2}, \quad \text{where } \mathcal{R}[\xi](\mathbf{x}) = \xi(R^*\mathbf{x}) = \xi(\mathbf{x}). \quad \text{(A5)}$$

Note that the above definition of bulk honeycomb media includes structures that are more general than just an ordinary honeycomb lattice of discrete sites. Any structure that satisfies the symmetries (e.g. a triangular lattice of pillars) is included in the definition.

[1] Note that, in the main text, we use Dirac notation for inner products $\langle f | g \rangle = \langle f, g \rangle$. Throughout the appendices, we will use the latter notation.

3. Dirac points

A Dirac point is an energy / quasi-momentum pair, $(E_D, \mathbf{K}_\star)$, at which there is a conical intersection of consecutive dispersion surfaces $E_-(\mathbf{k}) \leq E_+(\mathbf{k})$:

$$E_\pm(\mathbf{k}) - E_D \ = \pm \mathrm{v_D}\ |\mathbf{k} - \mathbf{K}_\star|\ (\ 1\ +\ O\left(|\mathbf{k} - \mathbf{K}_\star|\right)\ )$$

as $|\mathbf{k} - \mathbf{K}_\star| \to 0 \quad (\mathrm{v}_D > 0)$. In Fig. 5, we show the honeycomb photonic crystal discussed in the main text along with its band structure, which exhibits a Dirac point between the first and second TE bands.

Theorem A.2 *Generic bulk honeycomb operators of the type $\mathcal{L}_{\xi,\rho}$ (see* (A4)*) have Dirac points at the vertices of the Brillouin zone.*

See [30, 31] for the Schrödinger case and [32] for the Maxwell case. In the following discussion, we shall follow the mathematical formulations of these references.

4. Characterization of Dirac points

Let

$$L^2_{\mathbf{k}} \ = \ \Big\{ f : f(\mathbf{x}+\mathbf{v}) = e^{i\mathbf{k}\cdot\mathbf{v}} f(\mathbf{x}), \int_\Omega |f(\mathbf{x})|^2\ \rho(\mathbf{x})\ d\mathbf{x} < \infty \Big\} \qquad \text{(A6)}$$

where Ω = unit cell. The inner product on $L^2_{\mathbf{k}}$ is given by:

$$\langle f, g \rangle_\rho \ = \ \int_\Omega \overline{f(\mathbf{x})} g(\mathbf{x})\ \rho(\mathbf{x})\ d\mathbf{x}. \qquad \text{(A7)}$$

It will also be useful to introduce the standard L^2 inner product on a unit cell, which we denote by:

$$\langle f, g \rangle \ = \ \int_\Omega \overline{f(\mathbf{x})} g(\mathbf{x})\ d\mathbf{x}. \qquad \text{(A8)}$$

Introduce the subspaces $L^2_{\mathbf{K}_\star,\sigma}$ for $\sigma = 1, \tau, \bar{\tau}$ given by

$$L^2_{\mathbf{K}_\star,\sigma} \ = \ \Big\{ f : f \in L^2_{\mathbf{K}_\star},\ \mathcal{R}[f] = \sigma f \Big\}. \qquad \text{(A9)}$$

These are the three subspaces associated with the three distinct eigenvalues of $2\pi/3$ rotations. Then, we have an orthogonal decomposition of $L^2_{\mathbf{K}_\star}$:

$$L^2_{\mathbf{K}_\star} \ = \ L^2_{\mathbf{K}_\star,1} \oplus L^2_{\mathbf{K}_\star,\tau} \oplus L^2_{\mathbf{K}_\star,\bar{\tau}}$$

For any vertex $\mathbf{K}_\star$ of the Brillouin zone, $[\mathcal{R}, L_{\xi,\rho}]$ acts in $L^2_{\mathbf{K}_\star}$ and vanishes. Hence, we may study the bulk honeycomb operator, L_B, on each summand subspace (i.e., its eigenstates may be chosen to reside within the subspaces introduced above). We have the following characterization of Dirac points.

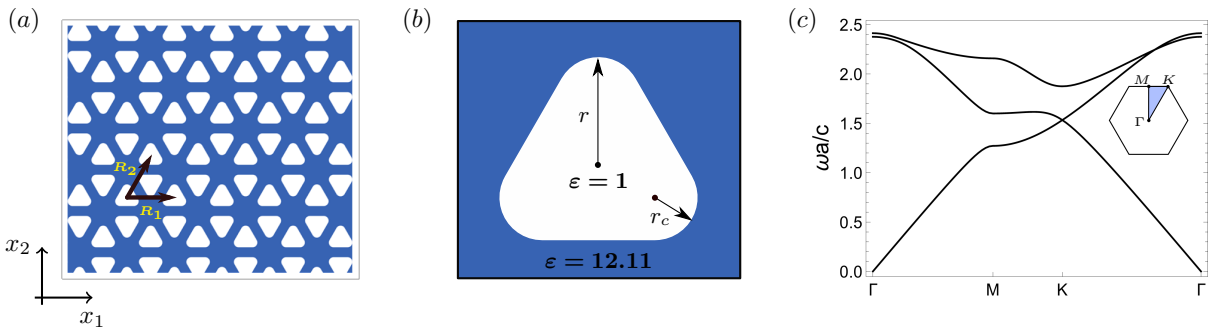

FIG. 5. Illustration of the unstrained honeycomb photonic crystal discussed in the main text. (a) A portion of the periodic structure consisting of triangular air holes embedded in silicon. Shown also are the lattice vectors $\mathbf{R}_1 = a[1, 0]$ and $\mathbf{R}_2 = a[1/2, \sqrt{3}/2]$. (b) Enlarged view of a single triangular air hole highlighting the values of the dielectric as well as the parameters r and r_c discussed in the main text. (c) TE bands of the structure, showing the Dirac point occurring between the first and second bands. Inset shows the Brillouin zone.

Proposition A.3 *Let $\mathcal{L}_{\xi,\rho}$ be as defined in* (A4). *Let $\mathbf{K}_\star = \mathbf{K}$ or $\mathbf{K}'$, the two independent high-symmetry vertex quasi-momenta of $\mathcal{B}$. The energy / quasi-momentum pair $(E_D, \mathbf{K}_\star)$ is a Dirac point (conical point) of $\mathcal{L}_{\xi,\rho}$ if:*

- *E_D is a simple $L^2_{\mathbf{K}_\star,\tau}$ eigenvalue of $\mathcal{L}_{\xi,\rho}$ with corresponding eigenstate $\Phi_1(\mathbf{x})$ satisfying: $\mathcal{L}_{\xi,\rho}\Phi_1 = E_D\Phi_1$, $\mathcal{R}[\Phi_1] = \tau\ \Phi_1$.*
- *E_D is a simple $L^2_{\mathbf{K}_\star,\overline{\tau}}$ eigenvalue of $\mathcal{L}_{\xi,\rho}$ with corresponding eigenstate $\Phi_2(\mathbf{x})$ satisfying: $\mathcal{L}_{\xi,\rho}\Phi_2 = E_D\Phi_2$, $\mathcal{R}[\Phi_2] = \overline{\tau}\ \Phi_2$.*
- *Φ_1 and Φ_2 are related by:*

$$\Phi_2(\mathbf{x}) = (\mathcal{PC})\,[\Phi_1](\mathbf{x}) = \overline{\Phi_1(-\mathbf{x})} \qquad \text{and} \quad \langle \Phi_j, \Phi_l \rangle_\rho = \delta_{jl}. \tag{A10}$$

- *E_D is not a $L^2_{\mathbf{K}_\star,1}$ eigenvalue of $\mathcal{L}_{\xi,\rho}$.*

Furthermore, when the above conditions hold, we have the following: Let $\Phi_j^{\mathbf{K}_\star}$, $j = 1, 2$ denote the pair of eigensolutions for $\mathbf{K}_\star = \mathbf{K}$ or $\mathbf{K}'$. Then, for some constant, v_D, we have

$$\left\langle \Phi_1^{\mathbf{K}}, \mathcal{A}\Phi_2^{\mathbf{K}} \right\rangle \ = \ \mathrm{v}_D \begin{pmatrix} 1 \\ i \end{pmatrix}, \tag{A11}$$

where $\mathcal{A}$ is given by:

$$\mathcal{A} \ = \ \frac{1}{i}\nabla_{\mathbf{y}}\,(\xi(\mathbf{y})\cdot) \ + \ \xi(\mathbf{y})\frac{1}{i}\nabla_{\mathbf{y}}\,. \tag{A12}$$

See Theorem 4.1 of [30], Theorem 2 of [32] and Section 3.1 of [27].

Remark A.4 *Note that if Φ_1 and Φ_2 are a choice of Bloch modes for the Dirac point $(E_D, \mathbf{K}_\star)$ satisfying all conditions of Proposition A.3, then so are $e^{i\phi}\Phi_1$ and $e^{-i\phi}\Phi_2$ for any $\phi \in \mathbb{R}$. We shall take advantage of this degree of freedom in the proof of Proposition A.5, where we choose a phase convention and coordinate system in which our effective equations take on a simplified form.*

Proposition A.5 *There is a coordinate system and a phase convention for the states Φ_1 and Φ_2 such that:*

$$\mathrm{v}_D = \langle \Phi_1, \mathcal{A}_1\Phi_2 \rangle \geq 0 \tag{A13}$$

$$b_\star \ \equiv \ \langle \partial_{x_1}\Phi_1,\ \xi\ \partial_{x_1}\Phi_2 \rangle \ \geq \ 0. \tag{A14}$$

The proof of Proposition A.5 is given in Appendix F. It is dependent on Proposition C.3 in Section C, where the expression $b_\star$ arises in the derivation of the effective Hamiltonian. Henceforth, we shall assume throughout that $\mathrm{v}_D > 0$ and $b_\star > 0$.

We note that, for the structure studied numerically in the main text, the choice of coordinate system illustrated in Fig. 5(a) (paired with an appropriate choice of phase convention) was found from numerical simulations to produce a real-valued v_D and $b_\star$. We also note that in [30, 32] it is shown that v_D is generically non-zero. We believe that the same techniques can be used to show that both v_D and $b_\star$ are generically non-zero.

Appendix B: The deformed bulk honeycomb medium

We start with a bulk honeycomb (unstrained) medium, whose modes are solutions to the eigenvalue problem:

$$(\ -\nabla_{\mathbf{x}}\cdot\xi(\mathbf{x})\nabla_{\mathbf{x}} \ + \ V(\mathbf{x})\ )\psi \ = \ E\rho(\mathbf{x})\psi \tag{B1}$$

We subject the medium to a strain which is non-uniform on a length scale which is large compared with the lattice constant of the structure, denoted a:

$$\mathbf{x} \mapsto T(\mathbf{x}) \ \equiv \ \mathbf{x} \ + \ \mathbf{u}(\kappa\mathbf{x}), \quad \kappa a \ll 1,$$

where $\mathbf{u}(\mathbf{X}) = (u_1(\mathbf{X}), u_2(\mathbf{X}))$ and $\mathbf{X} = (X_1, X_2)$ [2]. The Jacobian of T is given by $D_{\mathbf{x}}T(\mathbf{x}) = I_{2\times 2} +$

[2] Here we take the deformation to be of the form $\mathbf{u}(\kappa\mathbf{x})$ instead of $\mathbf{u}(x)$ (compare with the main text). In doing so we are explicitly introducing the small parameter measuring the size of the deformation in order to facilitate our systematic perturbation theory.

$\kappa D_{\mathbf{X}}\mathbf{u}(\mathbf{X})\Big|_{\mathbf{X}=\kappa\mathbf{x}}$, where:

$$\big[D_{\mathbf{X}}\mathbf{u}(\mathbf{X})\big]_{jl} \;\equiv\; \Big(\frac{\partial u_j(X_1,X_2)}{\partial X_l}\Big)_{j,l=1,2} \;\equiv\; (u_{j,l})_{j,l=1,2} \tag{B2}$$

is the 2×2 Jacobian matrix. If $\|D_{\mathbf{X}}\mathbf{u}(\mathbf{X})\|$ is bounded, then T is invertible for κ small.

We note that the deformation that we choose later on (corresponding to a constant pseudo-magnetic field) arises from a strain that grows linearly: $\big|\big(D_{\mathbf{X}}\mathbf{u}(\mathbf{X})\big)_{jl}\big| \sim a|\mathbf{X}|$. In this case, our asymptotic analysis is, strictly speaking, no longer valid at large distances: $|\mathbf{X}| \gg (\kappa a)^{-1}$. However, near the center of the band at $k_y a' = 0$ (see Fig. 2(b) of the main text), the Landau level wavefunctions are localized near $\mathbf{X} = \mathbf{0}$, and thus are supported only where the strain is weak. We therefore expect the $\mathcal{O}(\kappa)$ asymptotic analysis to be accurate up to $\mathcal{O}(\kappa^2)$ corrections in this regime (i.e. for $\mathbf{X} \approx \mathbf{0}$ and $k_y a'$ close to 0) [3].

The deformed medium is defined by primed material relations:

$$\begin{aligned}\xi'(T(\mathbf{x})) &= \xi(\mathbf{x})\\ V'(T(\mathbf{x})) &= V(\mathbf{x})\\ \rho'(T(\mathbf{x})) &= \rho(\mathbf{x}).\end{aligned}$$

Assuming that T is invertible, we have

$$\begin{aligned}\xi'(\mathbf{x}) &= \xi(T^{-1}(\mathbf{x}))\\ V'(\mathbf{x}) &= V(T^{-1}(\mathbf{x}))\\ \rho'(\mathbf{x}) &= \rho(T^{-1}(\mathbf{x})).\end{aligned}$$

The spectral problem governing modes of the deformed medium is then:

$$\big(\, -\nabla_{\mathbf{x}}\cdot\xi'(\mathbf{x})\nabla_{\mathbf{x}} \;+\; V'(\mathbf{x})\,\big)\,\psi \;=\; E\rho'(\mathbf{x})\psi. \tag{B3}$$

Introducing the change of variables and definitions

$$\mathbf{y} \;=\; T^{-1}(\mathbf{x}) \tag{B4}$$

$$J(\mathbf{y}) \;\equiv\; D_{\mathbf{x}}T^{-1}(\mathbf{x})\Big|_{\mathbf{x}=T(\mathbf{y})} = [\partial_{\mathbf{y}}T(\mathbf{y})]^{-1} \tag{B5}$$

$$|J(\mathbf{y})| \;\equiv\; \det J(\mathbf{y}) \tag{B6}$$

we obtain an equivalent equation to (B3) in terms of the undeformed material functions:

$$-\left[|J(\mathbf{y})|\nabla_{\mathbf{y}}\cdot\frac{J(\mathbf{y})\xi(\mathbf{y})J^{\top}(\mathbf{y})}{|J(\mathbf{y})|}\,\nabla_{\mathbf{y}}\right]\,\psi + \;V(\mathbf{y})\;\psi \;=\; E\rho(\mathbf{y})\psi. \tag{B7}$$

For the undeformed problem, $\kappa = 0$, (B7) reduces to (B1).

We next expand the equation (B7) in the small parameter κ and drop terms of order κ^2 and higher order. For simplicity we consider the isotropic case:

$$\xi = \xi(\mathbf{x})I_{2\times 2}. \tag{B8}$$

Since $T(\mathbf{y}) = \mathbf{y} + \mathbf{u}(\kappa\mathbf{y})$, we have $D_{\mathbf{y}}T(\mathbf{y}) = I_{2\times 2} + \kappa D_{\mathbf{Y}}\mathbf{u}(\mathbf{Y})\Big|_{\mathbf{Y}=\kappa\mathbf{y}}$. Therefore,

$$\begin{aligned}J(\mathbf{y}) \;&=\; I_{2\times 2} \;-\kappa D_{\mathbf{Y}}\mathbf{u}(\mathbf{Y})\Big|_{\mathbf{Y}=\kappa\mathbf{y}} \;+\; \mathcal{O}(\kappa^2)\\ &=\; \begin{pmatrix}1-\kappa u_{1,1} & -\kappa u_{1,2}\\ -\kappa u_{2,1} & 1-\kappa u_{2,2}\end{pmatrix}\Big|_{\mathbf{Y}=\kappa\mathbf{y}} \;+\; \mathcal{O}(\kappa^2)\end{aligned} \tag{B9}$$

and

$$|J(\mathbf{y})| \;= 1 \;-\; \kappa\;\nabla_{\mathbf{Y}}\cdot\mathbf{u}(\mathbf{Y})\Big|_{\mathbf{Y}=\kappa\mathbf{y}} \;+\; \mathcal{O}(\kappa^2) \tag{B10}$$

We next expand (B7) using

$$\begin{aligned}|J|\nabla_{\mathbf{y}}\cdot\frac{J\xi J^{\top}}{|J|}\,\nabla_{\mathbf{y}} \;&=\; \nabla_{\mathbf{y}}\cdot J\xi J^{\top}\,\nabla_{\mathbf{y}} \;+\; |J|\,\big(\nabla_{\mathbf{y}}|J|^{-1}\,\big)\\ &\qquad\cdot\big(J\xi J^{\top}\,\nabla_{\mathbf{y}}\big)\\ &=\; \nabla_{\mathbf{y}}\cdot J\xi J^{\top}\,\nabla_{\mathbf{y}} \;+\; \mathcal{O}(\kappa^2)\end{aligned} \tag{B11}$$

and

$$\begin{aligned}J\xi J^{\top} \;&=\; (\;I_{2\times 2} - \kappa D_{\mathbf{Y}}u\;)\;\xi\;\big(\;I_{2\times 2} - \kappa(D_{\mathbf{Y}}u)^{\top}\;\big)\\ &\quad + \mathcal{O}(\kappa^2)\\ &=\; \xi \;-\; 2\,\kappa\,\xi\,U \;+\; \mathcal{O}(\kappa^2),\end{aligned} \tag{B12}$$

where $U = (U_{ij})$, the strain matrix, with entries [4]

$$\begin{aligned}U_{ij}(\mathbf{Y}) \;&=\; \frac{1}{2}\,\Big(\,\frac{\partial u_i}{\partial Y_j} \;+\; \frac{\partial u_j}{\partial Y_i}\,\Big)\\ &=\; \frac{1}{2}\,\big(\;D_{\mathbf{Y}}\mathbf{u}(\mathbf{Y}) \;+\; D_{\mathbf{Y}}\mathbf{u}(\mathbf{Y})^{\top}\;\big)_{ij}\end{aligned} \tag{B13}$$

Using (B11), (B12) and (B13) in (B7) yields:

$$\begin{aligned}&\big(\,-\nabla_{\mathbf{y}}\cdot\xi(\mathbf{y})\,\nabla_{\mathbf{y}} \;+\; V(\mathbf{y})\,\big)\,\psi\\ &\quad+\; 2\,\kappa\,\nabla_{\mathbf{y}}\cdot\xi(\mathbf{y})\,U(\kappa\mathbf{y})\,\nabla_{\mathbf{y}}\,\psi\\ &\quad=\; E\;\rho(\mathbf{y})\;\psi \;+\; \mathcal{O}(\kappa^2)\end{aligned} \tag{B14}$$

[3] We conjecture that a physical regularization of the structure (one in which the structure is undeformed for $|x_1|$ sufficiently large), will yield high density of states near the degenerate Landau levels of the present asymptotic theory. A mathematically rigorous treatment is work in progress.

[4] Since, in these appendices, we have explicitly introduced the small parameter κ, the κ dependence of the strain matrix has been made explicit and is factored out of U as defined above. The strain matrix defined in the main text thus differs from that defined here by a factor of κ and is given by κU.

Appendix C: Effective equations via multiscale analysis

1. Multiscale solutions

The form of the expanded Helmholtz / Schrödinger operator on the left-hand side of (B14) reflects the assumptions on our slowly deformed bulk structure; it depends on the two spatial scales: $\mathbf{y}$ (fast) and $\mathbf{Y} = \kappa\mathbf{y}$ (slow). To capture the κ^{-1} length scale effect of the non-uniform deformation, we seek solutions which explicitly incorporate both of these scales:

$$\psi^\kappa(\mathbf{y}) = \Psi^\kappa(\mathbf{y},\mathbf{Y})|_{\mathbf{Y}=\kappa\mathbf{y}}\,, \tag{C1}$$

where $\mathbf{y}$ and $\mathbf{Y}$ are to be treated as independent variables. Reflecting this, the solutions of (B14) that we shall construct are approximate wavepackets consisting of bulk Bloch mode components with energies nearby the Dirac point $|E - E_D| \lesssim C\kappa$. The expansion procedure we present has been made mathematically rigorous in many settings; in the context of perturbed honeycomb structures, see for example, [26, 27, 32].

First, we re-express (B14) in terms of this extended set of variables: $(\mathbf{y},\mathbf{Y})$. Thus we replace $\nabla_{\mathbf{y}}$ by $\nabla_{\mathbf{y}} + \kappa\nabla_{\mathbf{Y}}$ in (B14). Keeping terms of order κ^0 and κ^1, we find that (B14) becomes:

$$(\ \mathcal{L}_0 \ + \ \kappa\mathcal{L}_1\ )\ \Psi^\kappa(\mathbf{y},\mathbf{Y}) \ = \ E\ \rho\ \Psi^\kappa(\mathbf{y},\mathbf{Y}) \ + \ \mathcal{O}(\kappa^2)$$

where

$$\begin{aligned}
\mathcal{L}_0 \ &= \ -\nabla_{\mathbf{y}}\cdot\xi(\mathbf{y})\ \nabla_{\mathbf{y}} \ + \ V(\mathbf{y}) && \text{(C2)}\\
\mathcal{L}_1 \ &= \ -\ (\ \nabla_{\mathbf{y}}\cdot\xi(\mathbf{y})\nabla_{\mathbf{Y}} + \ \nabla_{\mathbf{Y}}\cdot\xi(\mathbf{y})\nabla_{\mathbf{y}}) \\
&\quad + \ 2\ \nabla_{\mathbf{y}}\cdot\xi(\mathbf{y})\ U(\mathbf{Y})\ \nabla_{\mathbf{y}} && \text{(C3)}
\end{aligned}$$

For each fixed $\mathbf{Y}\in\mathbb{R}^2$, the operators $\mathcal{L}_0$ and $\mathcal{L}_1$ are self-adjoint operators in $L^2_{\mathbf{K}}$.

We study the ($\mathcal{O}(\kappa)$ approximate) eigenvalue problem[5]

$$\begin{aligned}
&(\mathcal{L}_0 + \kappa\mathcal{L}_1)\,\Psi^\kappa = \ E\ \rho\ \Psi^\kappa, && \text{(C4)}\\
&\Psi^\kappa(\mathbf{y}+\mathbf{v},\mathbf{Y}) = e^{i\mathbf{K}\cdot\mathbf{v}}\ \Psi^\kappa(\mathbf{y},\mathbf{Y}), && \text{(C5)}\\
&\text{(with specified boundary conditions for} \\
&\Psi^\kappa(\mathbf{y},\mathbf{Y}) \text{ with respect to } \mathbf{Y}). && \text{(C6)}
\end{aligned}$$

Seek a solution of (C4)–(C6) as an expansion:

$$\begin{aligned}
\Psi^\kappa(\mathbf{y},\mathbf{Y}) \ &= \ \psi_0(\mathbf{y},\mathbf{Y}) + \kappa\psi_1(\mathbf{y},\mathbf{Y}) + \dots && \text{(C7)}\\
E^\kappa \ &= \ E_0 + \kappa E_1 + \dots && \text{(C8)}
\end{aligned}$$

[5] At this stage we do not specify boundary conditions with respect to $\mathbf{Y} = (Y_1, Y_2)$. These are specified below and depend on our choice of deformation. Specifically, for deformations giving rise to a Landau-gauge vector potential with constant effective magnetic field we shall choose: ψ to be pseudo-periodic with respect to Y_2 and decaying as $|Y_1|\to\infty$. See Section D.

where each $\psi_j(\mathbf{y},\mathbf{Y})$ satisfies the boundary conditions (C5)–(C6). Substitution and equating like powers of κ yields a hierarchy of equations. The first two of these are:

$$\begin{aligned}
\mathcal{O}(\kappa^0): \quad &(\ -\nabla_{\mathbf{y}}\cdot\xi(\mathbf{y})\ \nabla_{\mathbf{y}} \ + \ V(\mathbf{y}) - E_0\ \rho(\mathbf{y})\ )\,\psi_0 \\
&= \ 0 && \text{(C9)}\\
\mathcal{O}(\kappa^1): \quad &(\ -\nabla_{\mathbf{y}}\cdot\xi(\mathbf{y})\ \nabla_{\mathbf{y}} \ + \ V(\mathbf{y}) - E_0\ \rho(\mathbf{y})\ )\,\psi_1 \\
&= \ -\mathcal{L}_1\psi_0 + E_1\ \rho(\mathbf{y})\ \psi_0 && \text{(C10)}
\end{aligned}$$

The general solution, ψ_0, of (C9) with boundary conditions (C5)–(C6) is:

$$\psi_0(\mathbf{y},\mathbf{Y}) \ = \ \sum_{j=1}^{2}\alpha_j(\mathbf{Y})\Phi_j(\mathbf{y}), \quad E_0 = E_D \tag{C11}$$

where

(a) $\Phi_j(\mathbf{y})$, $j = 1,2$ span the two-dimensional $\mathbf{K}-$pseudoperiodic eigenspace of $\frac{1}{\rho(\mathbf{y})}\mathcal{L}_0$ with eigenvalue $E_0 = E_D$ (see Theorem A.2); and

(b) $\alpha_j(\mathbf{Y})$ are functions to be determined, which vary on the slow scale, $\mathbf{Y}$, and are chosen to satisfy the condition (C6) in $\mathbf{Y}$.

Using (C11), we have that (C10) becomes the non-homogeneous equation:

$$\begin{aligned}
&(-\nabla_{\mathbf{y}}\cdot\xi(\mathbf{y})\ \nabla_{\mathbf{y}} \ + \ V(\mathbf{y}) - E_D\ \rho(\mathbf{y})\ )\,\psi_1 \\
&\quad = \ \sum_{j=1}^{2}(-\mathcal{L}_1)\ (\ \alpha_j(\mathbf{Y})\Phi_j(\mathbf{y})\ ) \\
&\qquad + \ E_1\ \sum_{j=1}^{2}\ \alpha_j(\mathbf{Y})\ \rho(\mathbf{y})\Phi_j(\mathbf{y}) && \text{(C12)}
\end{aligned}$$

where ψ_1 satisfies the boundary conditions (C5)–(C6). Next, introduce the self-adjoint first order vector-operator

$$\begin{aligned}
\mathcal{A} \ &= \ \frac{1}{i}\nabla_{\mathbf{y}}\,(\xi(\mathbf{y})\cdot) \ + \ \xi(\mathbf{y})\frac{1}{i}\nabla_{\mathbf{y}}, \text{ or} \\
\mathcal{A} \ &= \ (\mathcal{A}_1,\mathcal{A}_2)\,, \text{ where } \quad \mathcal{A}_l \equiv \frac{1}{i}\partial_{y_l}\,(\xi(\mathbf{y})\cdot) \ + \ \xi(\mathbf{y})\frac{1}{i}\partial_{y_l} && \text{(C13)}
\end{aligned}$$

Then, the equation for ψ_1 may be rewritten as:

$$\begin{aligned}
&(-\nabla_{\mathbf{y}}\cdot\xi(\mathbf{y})\ \nabla_{\mathbf{y}} \ + \ V(\mathbf{y}) - E_D\ \rho(\mathbf{y})\ )\,\psi_1 \\
&= \ i\ \sum_{j=1}^{2}\mathcal{A}\Phi_j(\mathbf{y})\cdot\nabla_{\mathbf{Y}}\alpha_j(\mathbf{Y}) \\
&\quad - \ 2\ \sum_{j=1}^{2}\nabla_{\mathbf{y}}\cdot\xi(\mathbf{y})\ U(\mathbf{Y})\ \nabla_{\mathbf{y}}\Phi_j(\mathbf{y})\ \alpha_j(\mathbf{Y}) \\
&\quad + \ E_1\ \rho(\mathbf{y})\ \sum_{j=1}^{2}\Phi_j(\mathbf{y})\alpha_j(\mathbf{Y})\,. && \text{(C14)}
\end{aligned}$$

The non-homogeneous equation (C14) is viewed as an equation for $\mathbf{y} \mapsto \psi_1(\mathbf{y}, \mathbf{Y})$ satisfying the pseudoperiodic boundary condition (C5). A necessary and sufficient condition for solvability is that the right hand side of (C14) be L^2 orthogonal to the Dirac subspace of $\mathcal{L}_0 = -\nabla_{\mathbf{y}} \cdot \xi(\mathbf{y})\, \nabla_{\mathbf{y}} + V(\mathbf{y})$ at energy E_D, which is spanned by $\{\, \Phi_1, \Phi_2 \,\}$. Thus we have,

Proposition C.1 *Equation* (C14) *for* $\psi_1(\mathbf{y}, \mathbf{Y})$ *with boundary conditions* (C5)–(C6) *has a solution if and only if* $\alpha(\mathbf{Y}) = (\alpha_1(\mathbf{Y}), \alpha_2(\mathbf{Y}))^\top$ *satisfy the following eigenvalue problem for* $(\alpha(\mathbf{Y}), E_1)$ *subject to the boundary condition imposed in* (C6)*.*

$$
\begin{aligned}
&- i \sum_{j=1}^{2} \langle \Phi_l, \mathcal{A}\Phi_j \rangle \cdot \nabla_{\mathbf{Y}} \alpha_j(\mathbf{Y}) \\
&+ 2 \sum_{j=1}^{2} \langle \Phi_l, \nabla_{\mathbf{y}} \cdot \xi\, U(\mathbf{Y})\, \nabla_{\mathbf{y}} \Phi_j \rangle\ \alpha_j(\mathbf{Y}) \\
&= E_1\, \alpha_l(\mathbf{Y}), \quad \textit{for } l = 1, 2,
\end{aligned}
\tag{C15}
$$

where we have used the normalization $\langle \Phi_l, \rho\, \Phi_j \rangle = \delta_{lj}$*; see* (A10)*.*

We next write out explicitly the second term in (C15):

$$
\begin{aligned}
&2\ \langle \Phi_l, \nabla_{\mathbf{y}} \cdot \xi\, U(\mathbf{Y})\, \nabla_{\mathbf{y}} \Phi_j \rangle \\
&= -2\ \langle \nabla_{\mathbf{y}} \Phi_l, \xi\, U(\mathbf{Y})\, \nabla_{\mathbf{y}} \Phi_j \rangle \\
&= -2 \sum_m \left\langle\, \partial_{y_m} \Phi_l\ ,\ \xi \sum_n U_{mn}(\mathbf{Y})\, \partial_{y_n} \Phi_j \,\right\rangle \\
&= -2 \sum_{m,n} U_{mn}(\mathbf{Y})\ \langle\ \partial_{y_m} \Phi_l\ ,\ \xi\, \partial_{y_n} \Phi_j\ \rangle
\end{aligned}
\tag{C16}
$$

2. Simplification of the system (C15) via application of symmetries

Honeycomb symmetry enables simplification of the eigenvalue problem (C15) for the pair (α, E_1). The coefficients in (C15) are inner products of the form:

$$
\begin{aligned}
&\langle \Phi_l, \zeta \cdot \mathcal{A}\Phi_j \rangle \quad \text{and} \\
&A^{lj}_{\alpha\beta} = \left\langle \partial_{y_\alpha} \Phi_l, \xi\, \partial_{y_\beta} \Phi_j \right\rangle, \quad j, l, \alpha, \beta = 1, 2.
\end{aligned}
\tag{C17}
$$

We next discuss their simplification using symmetry arguments. These results are then applied in Section D to obtain our effective equations.

The first type of inner product in (C17) is evaluated using:

Proposition C.2 *For* $\zeta = (\zeta^{(1)}, \zeta^{(2)}) \in \mathbb{C}^2$*, we have*

1. $\langle \Phi_1, \zeta \cdot \mathcal{A}\Phi_1 \rangle = \langle \Phi_2, \zeta \cdot \mathcal{A}\Phi_2 \rangle = 0$.
2. $\langle \Phi_1, \zeta \cdot \mathcal{A}\Phi_2 \rangle = \overline{\langle \Phi_2, \zeta \cdot \mathcal{A}\Phi_1 \rangle} = \mathrm{v}_D\ (\zeta^{(1)} + i\zeta^{(2)})$, *where* $\mathrm{v}_D = \frac{1}{2} \langle \Phi_1, \mathcal{A}\Phi_2 \rangle \cdot (1, -i)$*; see* (A11)*.*

Proposition C.2 follows from Proposition A.3; see also [27, 30, 32]. The second type of inner product in (C17) is evaluated using the following proposition which is proved in Section E:

Proposition C.3 *Let* A^{lj}*, with entries* $A^{lj}_{\alpha\beta}$*, be as defined in* (C17)*:*

$$
A^{lj}_{\alpha\beta} = \left\langle \partial_{y_\alpha} \Phi_l, \xi\ \partial_{y_\beta} \Phi_j \right\rangle, \quad j, l, \alpha, \beta = 1, 2.
$$

Then,

1. *For* $l = j$*:*

$$
\begin{aligned}
A^{jj} &= a_\star\, I_{2\times 2} + \tilde{a}^{jj} \begin{pmatrix} 0 & 1 \\ -1 & 0 \end{pmatrix} \\
&= a_\star\, \sigma_0 + i\, \tilde{a}^{jj}\, \sigma_2,
\end{aligned}
\tag{C18}
$$

where $\tilde{a}^{jj}$ *are constants and* $a_\star \geq 0$ *and is given by*

$$
\begin{aligned}
a_\star &= \langle \partial_{y_1} \Phi_1, \xi\ \partial_{y_1} \Phi_1 \rangle \\
&= \langle \partial_{y_2} \Phi_1, \xi\ \partial_{y_2} \Phi_1 \rangle, \quad \text{and}
\end{aligned}
\tag{C19}
$$

$$
\begin{aligned}
a_\star &= \langle \partial_{y_1} \Phi_2,\ \xi\ \partial_{y_1} \Phi_2 \rangle \\
&= \langle \partial_{y_2} \Phi_2, \xi\ \partial_{y_2} \Phi_2 \rangle.
\end{aligned}
\tag{C20}
$$

Moreover,

$$
\begin{aligned}
a_\star &= \frac{1}{2}\, E_D - \frac{1}{2} \int_\Omega V(\mathbf{y}) |\Phi_j(\mathbf{y})|^2\, d\mathbf{y} \\
&\textit{with } j = 1 \text{ or } 2.
\end{aligned}
\tag{C21}
$$

2. *For* $l \neq j$*:*

$$
\begin{aligned}
A^{12} &= b_\star \begin{pmatrix} 1 & -i \\ -i & -1 \end{pmatrix} \\
&= b_\star\ (\ \sigma_3 - i\, \sigma_1\ ) \\
&\textit{where} \quad b_\star = \langle \partial_{y_1} \Phi_1, \xi\ \partial_{y_1} \Phi_2 \rangle
\end{aligned}
\tag{C22}
$$

$$
\begin{aligned}
A^{21} &= \overline{A^{12}} = \overline{b_\star} \begin{pmatrix} 1 & i \\ i & -1 \end{pmatrix} \\
&= \overline{b_\star}\ (\ \sigma_3 + i\, \sigma_1\ ).
\end{aligned}
\tag{C23}
$$

Recall that by Proposition A.5, a coordinate system and eigenstate phase convention can always be chosen for which: $\mathrm{v}_D \geq 0$ and $b_\star \geq 0$. The proof of Proposition C.3 is given in Appendix E.

Appendix D: Pseudo-magnetic field and the effective equations

1. The general effective equations

Using Proposition C.2 and Proposition C.3 we may greatly simplify the left hand side of (C15). The detailed calculations are presented in Section D 5; see, in particular, (D21), (D22), (D27) and (D28). This gives our main result:

Theorem D.1

1. *The eigenvalue problem* (C15) *for* (α, E_1) *reduces to the eigenvalue problem,* $\mathcal{H}\alpha = E_1\alpha$*, where* $\mathcal{H}$ *is a Dirac Hamiltonian with effective magnetic and electric potentials:*

$$\mathcal{H} = \mathrm{v}_D \Big[(-i\partial_{Y_1} - A_1) \sigma_1 - (-i\partial_{Y_2} - A_2) \sigma_2 \Big] + W_{\text{eff}}\ \sigma_0. \tag{D1}$$

The effective electric potential, W_{eff}*, and effective magnetic potential,* $\mathbf{A}_{\text{eff}} = (A_1, A_2)$*, are given by:*

$$\begin{aligned} W_{\text{eff}}(\mathbf{Y}) &= -2a_\star\ \mathrm{tr}\,(U(\mathbf{Y})\sigma_0) \\ &= -2a_\star\,(\partial_{Y_1}u_1 + \partial_{Y_2}u_2) \qquad \text{(D2)} \\ A_1(\mathbf{Y}) &= +\frac{2b_\star}{\mathrm{v}_D}\ \mathrm{tr}\,(U(\mathbf{Y})\sigma_3) \\ &= +\frac{2b_\star}{\mathrm{v}_D}\ (\partial_{Y_1}u_1 - \partial_{Y_2}u_2) \qquad \text{(D3)} \\ A_2(\mathbf{Y}) &= -\frac{2b_\star}{\mathrm{v}_D}\ \mathrm{tr}\,(U(\mathbf{Y})\sigma_1) \\ &= -\frac{2b_\star}{\mathrm{v}_D}\ (\partial_{Y_1}u_2 + \partial_{Y_2}u_1) \qquad \text{(D4)} \end{aligned}$$

where, $\mathrm{v}_D > 0$*,* $a_\star \geq 0$ *and* $b_\star > 0$ *are constants given in terms of Bloch modes* Φ_1*,* Φ_2*:*

$$\begin{aligned} \mathrm{v}_D &= \langle \Phi_1, \mathcal{A}_1\Phi_2\rangle > 0. \\ a_\star &= \frac{1}{2}\ E_D\ -\ \frac{1}{2}\ \int_\Omega V(\mathbf{y})\ |\Phi_j(\mathbf{y})|^2\ d\mathbf{y} \\ &= \langle \partial_{y_1}\Phi_j,\ \xi\ \partial_{y_1}\Phi_j\rangle \geq 0,\ j = 1 \text{ or } 2 \\ b_\star &= \langle \partial_{y_1}\Phi_1,\ \xi\ \partial_{y_1}\Phi_2\rangle > 0. \end{aligned}$$

2. *Equivalently, the eigenvalue problem* (D1) *may be expressed in terms of* $\alpha' \equiv \sigma_1\alpha = (\alpha_2, \alpha_1)^\top$ *and* $\mathcal{H}_{\text{eff}} \equiv \sigma_1\mathcal{H}\sigma_1^{-1}$ *as* $\mathcal{H}_{\text{eff}}\alpha' = E_1\alpha'$*, where*

$$\mathcal{H}_{\text{eff}}\ =\ \mathrm{v}_D\,(-i\nabla_{\mathbf{Y}} - \mathbf{A}_{\text{eff}})\cdot\sigma\ +\ W_{\text{eff}}\ \sigma_0. \tag{D5}$$

Remark D.2 *Note that for 2D electromagnetics* ($V(\mathbf{x}) \equiv 0$) *we have*

$$a_\star = \frac{1}{2}\ E_D\ =\ \frac{1}{2}\ \left(\frac{\omega_D}{c}\right)^2.$$

Remark D.3 *Part (2) of Theorem D.1 follows from part (1) and the observation that* $\sigma_1\sigma_2\sigma_1^{-1} = -\sigma_2$*, which implies that:*

$$\begin{aligned} \mathcal{H}_{\text{eff}} &= \sigma_1\Big(\mathrm{v}_D\Big[(-i\partial_{Y_1} - A_1)\,\sigma_1 - (-i\partial_{Y_2} - A_2)\,\sigma_2\Big] \\ &\qquad + W_{\text{eff}}\sigma_0\Big)\sigma_1^{-1} \\ &= \mathrm{v}_D\ \Big[(-i\partial_{Y_1} - A_1)\,\sigma_1 + (-i\partial_{Y_2} - A_2)\,\sigma_2\Big] \\ &\quad + W_{\text{eff}}\sigma_0 \\ &= \mathrm{v}_D\,(-i\nabla_{\mathbf{Y}} - \mathbf{A}_{\text{eff}})\cdot\sigma + W_{\text{eff}}\sigma_0 \end{aligned}$$

This is equivalent to a relabeling of the pair of eigenmodes at the Dirac point: $\Phi_1 \mapsto \Phi_2$ *and* $\Phi_2 \mapsto \Phi_1$*.*

2. Divergence-free deformations and Landau level spectrum

Suppose that we constrain the deformation $\mathbf{u}(\mathbf{Y})$ by: $\mathrm{tr}\,(\sigma_0 U) = \nabla_{\mathbf{Y}}\cdot\mathbf{u} = 0$. Hence, $W_{\text{eff}}(\mathbf{Y}) = 0$ and $\mathcal{H}_{\text{eff}}$ takes the simpler form:

$$\mathcal{H}_{\text{eff}}\ =\ \mathrm{v}_D\ \Big[(-i\partial_{Y_1} - A_1)\,\sigma_1 + (-i\partial_{Y_2} - A_2)\,\sigma_2 \Big]. \tag{D6}$$

Defining $\hat{\mathbf{p}} = (\hat{p}_1, \hat{p}_2) = (-i\partial_{Y_1}, -i\partial_{Y_2})$, we observe that $\mathcal{H}_{\text{eff}}^2$ is a diagonal operator. Indeed,

$$\begin{aligned} \mathcal{H}_{\text{eff}}^2\ &=\ \mathrm{v}_D^2\ \Big[\ (\hat{p}_1 - A_1)\sigma_1\ +\ (\hat{p}_2 - A_2)\sigma_2\ \Big]^2 \\ &=\ \mathrm{v}_D^2\ \Big[\ (\hat{p}_1 - A_1)^2\ +\ (\hat{p}_2 - A_2)^2 \\ &\qquad +\ (\hat{p}_1 - A_1)(\hat{p}_2 - A_2)\sigma_1\sigma_2 \\ &\qquad +\ (p_2 - A_2)(p_1 - A_1)\sigma_2\sigma_1\ \Big] \\ &=\ \mathrm{v}_D^2\ \Big[\ (\hat{\mathbf{p}} - \mathbf{A}_{\text{eff}})^2\ \sigma_0 +\ (\ \partial_{Y_2}A_1 - \partial_{Y_1}A_2\ )\ \sigma_3\ \Big]. \end{aligned}$$

Hence,

$$\mathcal{H}_{\text{eff}}^2\ = \mathrm{v}_D^2\ \Big[\ (\hat{\mathbf{p}} - \mathbf{A}_{\text{eff}})^2\ \sigma_0 +\ V_{\text{eff}}\ \sigma_3\ \Big]\ , \text{ where} \tag{D7}$$

$$V_{\text{eff}}\ =\ -\,[\nabla_{\mathbf{Y}}\times\mathbf{A}_{\text{eff}}]\cdot\hat{\mathbf{z}}\ =\ \partial_{Y_2}A_1\ -\ \partial_{Y_1}A_2. \tag{D8}$$

Now take $\mathbf{A}_{\text{eff}}$ to be a Landau gauge vector potential for a constant magnetic field: $\mathbf{A}_{\text{eff}} = -B_0\ (0, Y_1)$. Then, $\nabla\times\mathbf{A}_{\text{eff}} = -B_0\hat{\mathbf{z}}$. By (D3)–(D4), we must have:

$$\begin{aligned} A_1 &= +\frac{2b_\star}{\mathrm{v}_D}\,(u_{1,1} - u_{2,2})\ = 0 \\ A_2 &= -\frac{2b_\star}{\mathrm{v}_D}\,(u_{1,2} + u_{2,1})\ = -B_0\ Y_1. \end{aligned} \tag{D9}$$

We solve equations (D9) by taking:

$$\mathbf{u}(\mathbf{Y}) = (u_1(\mathbf{Y}), u_2(\mathbf{Y}))\ =\ \frac{\mathrm{v}_D\ B_0}{4b_\star}\ \left(0, Y_1^2\right). \tag{D10}$$

From the above results, we have

$$\mathcal{H}_{\text{eff}}^2 = \mathrm{v}_D^2\ \left[p_1^2\sigma_0 + (p_2 + B_0Y_1)^2\sigma_0 + B_0\sigma_3\right]. \tag{D11}$$

This yields two decoupled copies of the Landau gauge Hamiltonian for a particle in a magnetic field, with the copies respectively shifted in energy by $\pm B_0$. The spectrum of $\mathcal{H}_{\text{eff}}^2$ thus follows from the spectrum of a particle in a magnetic field [33] which, in Landau gauge, consists of a series of discretely spaced Landau levels $e_n(k_2)$, where the eigenvalues $e_n(k_2)$ are independent of k_2 (k_2 being the momentum associated with translation symmetry along Y_2) and are thus infinitely degenerate. At a fixed value of k_2, the spectrum of $\mathcal{H}_{\text{eff}}^2$ therefore consists of a collection of discretely spaced eigenvalues $\mathrm{v}_D^2\,[2B_0(n + 1/2) \pm B_0]$ with $n = 0, 1, 2, \ldots$, and corresponding eigenstates with centering $\propto k_2$. This is equivalent to a spectrum (at a fixed k_2) consisting of eigenvalues $2\mathrm{v}_D^2B_0n$, with $n = 0, 1, 2, \ldots$, where each eigenvalue

other than the $n = 0$ eigenvalue is two-fold degenerate ($n = 0$ having no degeneracy). Upon taking the square root, the two-fold degenerate pairs split into distinct positive and negative eigenvalues, yielding for the spectrum of $\mathcal{H}_{\text{eff}}$:

$$(E_1)_n = \pm\sqrt{2\mathrm{v}_D^2 B_0 n} \text{ with } n \in \{0, 1, 2, \dots\}. \quad \text{(D12)}$$

For the photonic crystal case, we can map the eigenvalue corrections $(E_1)_n$ to mode frequencies ω_n using: $(\omega/c)^2 = E = E_{\text{D}} + \kappa E_1 + \mathcal{O}(\kappa^2)$, and $E_{\text{D}} = (\omega_{\text{D}}/c)^2$. This yields

$$\omega_n = \omega_{\text{D}} \pm \frac{c^2 \mathrm{v}_D}{\sqrt{2}\omega_{\text{D}}} \sqrt{n\,|\mathbf{B}_{\text{eff}}(\kappa)|} + O(\kappa^2) \quad \text{(D13)}$$

with $n \in \{0, 1, 2, \dots\}$ and where $|\mathbf{B}_{\text{eff}}(\kappa)| = B_0\,\kappa^2$; see also the main text.

3. Relation between modes at K and K′

For $\mathbf{K}_\star = \mathbf{K}, \mathbf{K}'$, denote by $\mathcal{H}_{\text{eff}}^{\mathbf{K}_\star}$ the effective Hamiltonian (see (D6) for $\mathcal{H}_{\text{eff}}^{\mathbf{K}}$) arising from the mode expansion applied to the Dirac point at $\mathbf{K}_\star$. Our analysis shows that a deformation (D10) induces an effective vector potential, $\mathbf{A}_{\text{eff}}^{\mathbf{K}} = (A_1^{\mathbf{K}}, A_2^{\mathbf{K}})$, for which $\mathcal{H}_{\text{eff}}^{\mathbf{K}}$ has Landau levels E_1 with corresponding modes $(\alpha_2^{\mathbf{K}}, \alpha_1^{\mathbf{K}})$ determined by:

$$\mathrm{v}_D^{\mathbf{K}}\Big[\left(-i\partial_{Y_1} - A_1^{\mathbf{K}}\right)\sigma_1 + \left(-i\partial_{Y_2} - A_2^{\mathbf{K}}\right)\sigma_2\Big]\begin{pmatrix}\alpha_2^{\mathbf{K}}\\ \alpha_1^{\mathbf{K}}\end{pmatrix} = E_1\begin{pmatrix}\alpha_2^{\mathbf{K}}\\ \alpha_1^{\mathbf{K}}\end{pmatrix}. \quad \text{(D14)}$$

A Landau level obtained by solving (D14) seeds the expansion of a mode: $\psi^{\mathbf{K}} \approx \alpha_1^{\mathbf{K}}\Phi_1^{\mathbf{K}} + \alpha_2^{\mathbf{K}}\Phi_2^{\mathbf{K}} + \mathcal{O}(\kappa)$ with eigenvalue $E = E_D + \kappa E_1 + \mathcal{O}(\kappa^2)$. This mode is formed from the degenerate pair of states associated with the the Dirac point $(\mathbf{K}, E_D)$. In addition to this mode, there is a corresponding mode associated with the Dirac point $(\mathbf{K}', E_D)$, and this mode similarly has an expansion: $\psi^{\mathbf{K}'} \approx \alpha_1^{\mathbf{K}'}\Phi_1^{\mathbf{K}'} + \alpha_2^{\mathbf{K}'}\Phi_2^{\mathbf{K}'} + \mathcal{O}(\kappa)$. Note that the modes $\Phi_i^{\mathbf{K}}$ are related to the modes $\Phi_i^{\mathbf{K}'}$ by complex conjugation: $(\Phi_1^{\mathbf{K}'}, \Phi_2^{\mathbf{K}'}) = (\overline{\Phi_2^{\mathbf{K}}}, \overline{\Phi_1^{\mathbf{K}}})$. (The subscripts are interchanged because the τ and $\bar{\tau}$ subspaces are interchanged upon complex conjugation. The index 1 is associated with τ and the index 2 with $\bar{\tau}$.) The modes $\psi^{\mathbf{K}}$ and $\psi^{\mathbf{K}'}$ are in fact related by time-reversal symmetry and hence we can get one from the other by via complex conjugation. Taking the complex conjugate of $\psi^{\mathbf{K}}$ gives

$$\begin{aligned}\overline{\psi^{\mathbf{K}}} &\approx \overline{\alpha_1^{\mathbf{K}}}\ \overline{\Phi_1^{\mathbf{K}}} + \overline{\alpha_2^{\mathbf{K}}}\ \overline{\Phi_2^{\mathbf{K}}}\\ &= \overline{\alpha_1^{\mathbf{K}}}\ \Phi_2^{\mathbf{K}'} + \overline{\alpha_2^{\mathbf{K}}}\ \Phi_1^{\mathbf{K}'}\\ &= \alpha_2^{\mathbf{K}'}\ \Phi_2^{\mathbf{K}'} + \alpha_1^{\mathbf{K}'}\ \Phi_1^{\mathbf{K}'}. \end{aligned} \quad \text{(D15)}$$

Comparing the last two lines, we have that $(\alpha_1^{\mathbf{K}'}, \alpha_2^{\mathbf{K}'}) = (\overline{\alpha_2^{\mathbf{K}}}, \overline{\alpha_1^{\mathbf{K}}})$. Hence, to obtain the effective Hamiltonian governing the modes $(\alpha_1^{\mathbf{K}'}, \alpha_2^{\mathbf{K}'})$, we can simply take the complex conjugate of (D14), yielding (after using $\overline{\sigma_2} = -\sigma_2$)

$$\mathrm{v}_D^{\mathbf{K}}\Big[-\left(-i\partial_{Y_1} + A_1^{\mathbf{K}}\right)\sigma_1 + \left(-i\partial_{Y_2} + A_2^{\mathbf{K}}\right)\sigma_2\Big]\begin{pmatrix}\alpha_1^{\mathbf{K}'}\\ \alpha_2^{\mathbf{K}'}\end{pmatrix} = E_1\begin{pmatrix}\alpha_1^{\mathbf{K}'}\\ \alpha_2^{\mathbf{K}'}\end{pmatrix}. \quad \text{(D16)}$$

One can either leave this equation in the form shown in (D16) (i.e., with an extra sign multiplying the σ_1 term), or one can further simplify the equation to a form analogous to (D14). In particular, multiplying both sides of (D16) by σ_1 allows us to rewrite the equation as an eigenvalue problem for $\sigma_1(\alpha_1^{\mathbf{K}'}, \alpha_2^{\mathbf{K}'})^T = (\alpha_2^{\mathbf{K}'}, \alpha_1^{\mathbf{K}'})^T$, yielding (after using $\sigma_1\sigma_2 = -\sigma_2\sigma_1$)

$$-\mathrm{v}_D^{\mathbf{K}}\Big[\left(-i\partial_{Y_1} + A_1^{\mathbf{K}}\right)\sigma_1 + \left(-i\partial_{Y_2} + A_2^{\mathbf{K}}\right)\sigma_2\Big]\begin{pmatrix}\alpha_2^{\mathbf{K}'}\\ \alpha_1^{\mathbf{K}'}\end{pmatrix} = E_1\begin{pmatrix}\alpha_2^{\mathbf{K}'}\\ \alpha_1^{\mathbf{K}'}\end{pmatrix}. \quad \text{(D17)}$$

Using $\mathrm{v}_D^{\mathbf{K}'} = -\mathrm{v}_D^{\mathbf{K}}$, we then have

$$\mathrm{v}_D^{\mathbf{K}'}\Big[\left(-i\partial_{Y_1} + A_1^{\mathbf{K}}\right)\sigma_1 + \left(-i\partial_{Y_2} + A_2^{\mathbf{K}}\right)\sigma_2\Big]\begin{pmatrix}\alpha_2^{\mathbf{K}'}\\ \alpha_1^{\mathbf{K}'}\end{pmatrix} = E_1\begin{pmatrix}\alpha_2^{\mathbf{K}'}\\ \alpha_1^{\mathbf{K}'}\end{pmatrix} \quad \text{(D18)}$$

which is in a form analogous to (D14). Thus, we have the eigenvalue problem

$$\mathcal{H}_{\text{eff}}^{\mathbf{K}'}\begin{pmatrix}\alpha_2^{\mathbf{K}'}\\ \alpha_1^{\mathbf{K}'}\end{pmatrix} = E_1\begin{pmatrix}\alpha_2^{\mathbf{K}'}\\ \alpha_1^{\mathbf{K}'}\end{pmatrix} \quad \text{(D19)}$$

where the effective Hamiltonian is given by

$$\mathcal{H}_{\text{eff}}^{\mathbf{K}'} = \mathrm{v}_D^{\mathbf{K}'}\ (\ -i\nabla_{\mathbf{Y}}\ -\ \mathbf{A}_{\text{eff}}^{\mathbf{K}'}\ )\cdot\sigma \quad \text{(D20)}$$

and the effective vector potential $\mathbf{A}_{\text{eff}}^{\mathbf{K}'} \equiv (A_1^{\mathbf{K}'}, A_2^{\mathbf{K}'})$ is given by $\mathbf{A}_{\text{eff}}^{\mathbf{K}'} = -\mathbf{A}_{\text{eff}}^{\mathbf{K}}$. Since the effective vector potential in the $\mathbf{K}'$ valley is opposite in sign to that in the $\mathbf{K}$ valley, the associated pseudomagnetic field likewise differs by a sign:

$$\nabla \times \mathbf{A}_{\text{eff}}^{\mathbf{K}'} = +B_0\hat{\mathbf{z}} = -\nabla \times \mathbf{A}_{\text{eff}}^{\mathbf{K}}.$$

Note that, for the Landau gauge used in (D10), the Gaussian-decaying modes are centered at $\tilde{x}^{\mathbf{K}_\star} \sim B_0^{-1}k_2$. Since the effective magnetic fields for the $\mathbf{K}$ and $\mathbf{K}'$ modes are of opposite sign, we have

$$\tilde{x}^{\mathbf{K}'} = -\tilde{x}^{\mathbf{K}}.$$

4. Flattening weakly dispersive Landau levels using a modified strain

The effective theory predicts perfectly flat Landau levels. However, the Landau levels in Fig. 2 of the main

text have dispersion arising from terms that are higher order in κ. To mitigate this dispersion, we note that the effective theory indicates that adding a quadratic strain-induced potential will tend to give the Landau levels curvature. Heuristically, this can be seen by recalling, for the standard Landau gauge Hamiltonian for a particle in a uniform magnetic field, that the eigenstate at a given k_2 in a given Landau level is localized in the x_1 direction and centered on $\tilde{x}$, where $\tilde{x} \propto k_2$. Based on the k_2-dependent centering of these eigenstates, one would expect that introducing an x_1-dependent onsite effective electric potential would add a k_2-dependent shift to the band frequencies since an eigenstate at k_2 should only be sensitive to the value of the potential over the finite region within which the state is localized.

Can the introduction of such an additional strain can be used to counter the curvature arising from higher order terms? Answering this question requires going beyond our effective equations. We therefore use full numerical simulations to compute the effect of adding the heuristically motivated strain and find that the unwanted dispersion can indeed be mitigated. As discussed in the main text, we modify the displacement to be $\mathbf{u}(\kappa\mathbf{x}) = a[\beta(\kappa x_1)^3, (\kappa x_1)^2]$, yielding a pseudo-magnetic field $\mathbf{B}(\mathbf{x}) = -(4a\kappa^2 b_\star/\mathrm{v}_D)\hat{\mathbf{z}}$ as well as a quadratic potential $W_{\text{eff}}(\mathbf{x}) = 3a\beta\kappa(\omega_D/c)^2(\kappa x_1)^2$. Taking $\kappa = 0.0548a^{-1}$ and $\beta = 0.0380$ yields the band structures shown in Fig. 4 of the main text, where we see a clear flattening of the Landau levels.

5. Proof of Theorem D.1 by simplification of (C15)

We next evaluate the terms in (C15), one at a time, using Proposition C.2 and Proposition C.3.

Term 1 of (C15), $l = 1$:

$$-i \sum_{j=1}^{2} \langle \Phi_1, \mathcal{A}\Phi_j \rangle \cdot \nabla_{\mathbf{Y}} \alpha_j = -i \langle \Phi_1, \mathcal{A}\Phi_2 \rangle \cdot \nabla_{\mathbf{Y}} \alpha_2 = \mathrm{v}_D \, (-i\partial_{Y_1} + \partial_{Y_2}) \, \alpha_2 \tag{D21}$$

Term 1 of (C15), $l = 2$:

$$-i \sum_{j=1}^{2} \langle \Phi_2, \mathcal{A}\Phi_j \rangle \cdot \nabla_{\mathbf{Y}} \alpha_j = -i \langle \Phi_2, \mathcal{A}\Phi_1 \rangle \cdot \nabla_{\mathbf{Y}} \alpha_1 = \mathrm{v}_D \, (-i\partial_{Y_1} - \partial_{Y_2}) \, \alpha_1 \tag{D22}$$

Term 2 of (C15), $l = 1$:

$$\begin{aligned} -2 \, \langle \Phi_1, \nabla_{\mathbf{y}} \cdot \xi \, U(\mathbf{Y}) \, \nabla_{\mathbf{y}} \Phi_j \rangle &= 2 \sum_{m,n} U_{mn}(\mathbf{Y}) \, \langle \, \partial_{y_m} \Phi_1 \, , \, \xi \, \partial_{y_n} \Phi_j \, \rangle && \text{(D23)} \\ &= 2 \sum_{m,n} U_{mn}(\mathbf{Y}) \, A^{1j}_{mn} && \text{(D24)} \end{aligned}$$

where we have used (C16) and the definition of A^{lj}_{mn} in (C17). Therefore,

$$2 \sum_j \langle \Phi_1, \nabla_{\mathbf{y}} \cdot \xi \, U(\mathbf{Y}) \, \nabla_{\mathbf{y}} \Phi_j \rangle \, \alpha_j(\mathbf{Y}) = -2 \sum_{m,n} U_{mn}(\mathbf{Y}) \sum_j A^{1j}_{mn} \, \alpha_j(\mathbf{Y}) \tag{D25}$$

Consider now the sum over j: $\sum_j A^{1j}_{mn} \, \alpha_j(\mathbf{Y}) = A^{11}_{mn}\alpha_1(\mathbf{Y}) + A^{12}_{mn}\alpha_2(\mathbf{Y})$. By Proposition C.3:

$$\begin{aligned} A^{11}_{mn} &= \left(\, a_\star \, \sigma_0 \, + \tilde{a}^{11} \, i\sigma_2 \, \right)_{mn} \quad \text{and} \\ A^{12}_{mn} &= b_\star \, \left(\, \sigma_3 \, - \, i \, \sigma_1 \, \right)_{mn} . \end{aligned}$$

Therefore,

$$\sum_j A^{1j}_{mn} \, \alpha_j(\mathbf{Y}) = \left(\, a_\star \, \sigma_0 \, + \tilde{a}^{11} \, i\sigma_2 \, \right)_{mn} \, \alpha_1(\mathbf{Y}) + \, b_\star \, \left(\, \sigma_3 \, - \, i \, \sigma_1 \, \right)_{mn} \, \alpha_2(\mathbf{Y}) \tag{D26}$$

and finally we have:

Term 2 of (C15), $l = 1$:

$$\begin{aligned} 2 \sum_j \langle \Phi_1, \nabla_{\mathbf{y}} \cdot \xi \, U(\mathbf{Y}) \, \nabla_{\mathbf{y}} \Phi_j \rangle \, \alpha_j(\mathbf{Y}) &= -2 \sum_{m,n} U_{mn}(\mathbf{Y}) \sum_j A^{1j}_{mn} \, \alpha_j(\mathbf{Y}) \\ &= -2 \sum_{m,n} U_{mn} \, \left(\, a_\star \, \sigma_0 \, + \tilde{a}^{11} \, i\sigma_2 \, \right)_{mn} \, \alpha_1 \\ &\quad - 2 \, b_\star \sum_{m,n} U_{mn} \, \left(\, \sigma_3 \, - \, i \, \sigma_1 \, \right)_{mn} \, \alpha_2 \\ &= -2 \, a_\star \, \mathrm{tr}(U) \, \alpha_1 \\ &\quad - 2 \, b_\star \, \left(\, \mathrm{tr}(\sigma_3 U) \, - \, i \, \mathrm{tr}(\sigma_1 U) \, \right) \, \alpha_2, \end{aligned} \tag{D27}$$

where we have used: $\sigma_2^\top = -\sigma_2$, $U^\top = U$ and finally $\mathrm{tr}(V^\top U) = \sum_{m,n} V_{mn} U_{mn}$. Similarly, we have for

Term 2 of (C15), $l = 2$:

$$\begin{aligned} 2 \sum_j \langle \Phi_2, \nabla_{\mathbf{y}} \cdot \xi \, U(\mathbf{Y}) \, \nabla_{\mathbf{y}} \Phi_j \rangle \, \alpha_j(\mathbf{Y}) &= -2 \sum_{m,n} U_{mn}(\mathbf{Y}) \sum_j A^{2j}_{mn} \, \alpha_j(\mathbf{Y}) \\ &= -2 \, a_\star \, \mathrm{tr}(U) \, \alpha_2 \\ &\quad - 2 \, b_\star \, \left(\, \mathrm{tr}(\sigma_3 U) + \, i \, \mathrm{tr}(\sigma_1 U) \, \right) \alpha_1. \end{aligned} \tag{D28}$$

We now complete the proof of Theorem D.1. Substitution of (D21) and (D27) into (C15) for $l = 1$, and (D22) and (D28) into (C15) for $l = 2$ yields the system:

$$\begin{aligned} &\left[\mathrm{v}_D(-i\partial_{Y_1} + \partial_{Y_2}) - 2b_\star \left(\mathrm{tr}(\sigma_3 U) - i\mathrm{tr}(\sigma_1 U) \right) \right] \alpha_2 \\ &\quad - 2a_\star \mathrm{tr}(U)\alpha_1 = E_1 \alpha_1 \\ &\left[\overline{\mathrm{v}_D}(-i\partial_{Y_1} - \partial_{Y_2}) - 2\overline{b_\star} \left(\mathrm{tr}(\sigma_3 U) + i\mathrm{tr}(\sigma_1 U) \right) \right] \alpha_1 \\ &\quad - 2a_\star \mathrm{tr}(U)\alpha_2 = E_1 \alpha_2, \end{aligned} \tag{D29}$$

where we recall from Proposition A.5 that $\mathrm{v}_D = \overline{\mathrm{v}_D}$ and $b_\star = \overline{b_\star}$. Using Pauli matrices, σ_i, the system (D29) can be expressed as (D1).

Appendix E: Matrix elements via symmetry; proof of Proposition C.3

Let $\mathbf{x} \mapsto R\mathbf{x}$ denote a rotation on $\mathbb{R}^2$ by $2\pi/3$

$$R \;=\; \begin{pmatrix} -\frac{1}{2} & \frac{\sqrt{3}}{2} \\ -\frac{\sqrt{3}}{2} & -\frac{1}{2} \end{pmatrix}$$

and recall the rotation operator: $\mathcal{R}[f](\mathbf{x}) \;=\; f(R^*\mathbf{x})$. Recall from Proposition A.3 that

$$\mathcal{R}[\Phi_j](\mathbf{x}) \;=\; \tau^j \Phi_j(\mathbf{x}),\; j=1,2, \text{ where } \tau = e^{2\pi i/3}.$$

Proposition E.1 *Let A^{ij} $(i,j=1,2)$ denote the matrices given in* (C17)*. Then,*

1. *For any i,j: $A^{ij} \;=\; \tau^{j-i}\; R^\top A^{ij} R$*
2. *$i=j$: $A^{jj} \;=\; R^\top A^{jj} R$*
3. *$i \neq j$: $A^{12} \;=\; \tau\; R^\top A^{12} R$, and $A^{21} \;=\; \overline{\tau}\; R^\top A^{21} R$*

Proof of Proposition E.1: Fix $\kappa = (\kappa_1, \kappa_2) \in \mathbb{R}^2$. Then, with summation over repeated indices implied,

$$\begin{aligned}
\kappa^\top\; A^{ij}\; \kappa \;&=\; \left\langle \partial_{y_\alpha}\Phi_i, \xi\; \partial_{y_\beta}\Phi_j \right\rangle\; \kappa_\alpha\kappa_\beta \\
&=\; \left\langle \mathcal{R}\; \partial_{y_\alpha}\Phi_i, \xi\; \mathcal{R}\; \partial_{y_\beta}\Phi_j \right\rangle\; \kappa_\alpha\kappa_\beta \\
&=\; \left\langle\; R_{n\alpha}\partial_{y_n}\; \mathcal{R}[\Phi_i], \xi\; R_{q\beta}\partial_{y_q}\; \mathcal{R}[\Phi_j] \right\rangle\; \kappa_\alpha\kappa_\beta \\
&=\; \left\langle\; R_{n\alpha}\partial_{y_n}\; \tau^i\Phi_i, \xi\; R_{q\beta}\partial_{y_q}\; \tau^j\Phi_j \right\rangle\; \kappa_\alpha\kappa_\beta \\
&=\; \tau^{j-i}\; \left\langle\; R_{n\alpha}\partial_{y_n}\; \Phi_i, \xi\; R_{q\beta}\partial_{y_q}\; \Phi_j \right\rangle\; \kappa_\alpha\kappa_\beta \\
&=\; \tau^{j-i}\; \left\langle\; \partial_{y_n}\; \Phi_i, \xi\; \partial_{y_q}\; \Phi_j \right\rangle\; R_{n\alpha}\kappa_\alpha\; R_{q\beta}\kappa_\beta \\
&=\; \tau^{j-i}\; \left\langle\; \partial_{y_n}\; \Phi_i, \xi\; \partial_{y_q}\; \Phi_j \right\rangle\; (R\kappa)_n\; (R\kappa)_q \\
&=\; \tau^{j-i}\; \left(R\kappa\right)^\top\; A^{ij} (R\kappa) \\
&=\; \tau^{j-i}\; \kappa^\top\; \left(\; R^\top A^{ij} R\; \right) \kappa
\end{aligned}$$

Since κ is arbitrary, we conclude:

$$A^{ij} \;=\; \tau^{j-i}\; R^\top A^{ij} R, \qquad i,j=1,2.$$

We have three cases:

$$\begin{cases} i=j: & A^{jj} \;=\; R^\top A^{jj} R, \quad j=1,2 \\ (i,j)=(1,2): & A^{12} \;=\; \tau\; R^\top A^{12} R \\ (i,j)=(2,1): & A^{21} \;=\; \overline{\tau}\; R^\top A^{21} R \end{cases} \tag{E1}$$

This completes the proof of Proposition E.1.

We now deduce Proposition C.3 using Proposition E.1.

Proof of Proposition C.3: The $2\pi/3$ rotation matrix is given by

$$R \;=\; \begin{pmatrix} -\frac{1}{2} & \frac{\sqrt{3}}{2} \\ -\frac{\sqrt{3}}{2} & -\frac{1}{2} \end{pmatrix} \tag{E2}$$

Case 1, i=j: By (E1) we have

$$\begin{pmatrix} -\frac{1}{2} & \frac{\sqrt{3}}{2} \\ -\frac{\sqrt{3}}{2} & -\frac{1}{2} \end{pmatrix} \begin{pmatrix} a & b \\ c & d \end{pmatrix} \;=\; \begin{pmatrix} a & b \\ c & d \end{pmatrix} \begin{pmatrix} -\frac{1}{2} & \frac{\sqrt{3}}{2} \\ -\frac{\sqrt{3}}{2} & -\frac{1}{2} \end{pmatrix},$$

where a, b, c and d are to be determined. Equating entries, yields that $c=-b$ and $a=d$. Hence,

$$A^{jj} \;=\; a^{jj}\; I_{2\times 2} \;+\; \tilde{a}^{jj}\; \begin{pmatrix} 0 & 1 \\ -1 & 0 \end{pmatrix}, \quad j=1,2.$$

We claim further that $a^{11} = a^{22}$. Indeed, we have:

$$\begin{aligned}
a^{11} \;&=\; \int_\Omega \overline{\frac{\partial\Phi_1(\mathbf{x})}{\partial x_1}}\; \xi(\mathbf{x})\; \frac{\partial\Phi_1(\mathbf{x})}{\partial x_1}\; d\mathbf{x} \\
&=\; \int_\Omega \overline{\frac{\partial\Phi_1(-\mathbf{y})}{\partial y_1}}\; \xi(-\mathbf{y})\; \frac{\partial\Phi_1(-\mathbf{y})}{\partial y_1}\; d\mathbf{y} \\
&=\; \int_\Omega \overline{\frac{\partial\Phi_1(-\mathbf{y})}{\partial y_1}}\; \xi(-\mathbf{y})\; \overline{\frac{\partial\overline{\Phi_1(-\mathbf{y})}}{\partial y_1}}\; d\mathbf{y} \\
&=\; \int_\Omega \frac{\partial\Phi_2(\mathbf{y})}{\partial y_1}\; \xi(\mathbf{y})\; \overline{\frac{\partial\Phi_2(\mathbf{y})}{\partial y_1}}\; d\mathbf{y} \;=\; a^{22}.
\end{aligned}$$

We therefore set $a_\star \equiv a^{11} \;=\; a^{22}$. Finally, taking the inner product of the equation $(-\nabla\cdot\xi\nabla \;+V)\,\Phi_j = E\;\rho\;\Phi_j$ with Φ_j and using that $\langle\Phi_i,\Phi_j\rangle_\rho = \delta_{ij}$ gives:

$$\int_\Omega \xi(\mathbf{y})\; |\nabla\Phi_j(\mathbf{y})|^2\; d\mathbf{y} \;+\; \int_\Omega V(\mathbf{y})\; |\Phi_j(\mathbf{y})|^2\; d\mathbf{y} = \;\; E_D \tag{E3}$$

with $j=1,2$. Hence,

$$a_\star \;=\; \frac{1}{2}\; E_D \;-\; \frac{1}{2}\; \int_\Omega V(\mathbf{y})\; |\Phi_j(\mathbf{y})|^2\; d\mathbf{y}\;,\; j=1,2. \tag{E4}$$

This proves (C19), (C20) and (C21), and in conclusion we have:

$$A^{jj} \;=\; a_\star\; I_{2\times 2} \;+\; \tilde{a}^{jj}\; \begin{pmatrix} 0 & 1 \\ -1 & 0 \end{pmatrix}, \quad j=1,2\;,$$

where $\tilde{a}^{22} = -\tilde{a}^{11}$. This proves part (1) of Proposition C.3.

Case 2, (i,j)=(1,2): By (E1) we have

$$\begin{pmatrix} -\frac{1}{2} & \frac{\sqrt{3}}{2} \\ -\frac{\sqrt{3}}{2} & -\frac{1}{2} \end{pmatrix} \begin{pmatrix} a & b \\ c & d \end{pmatrix} \;=\; \tau \begin{pmatrix} a & b \\ c & d \end{pmatrix} \begin{pmatrix} -\frac{1}{2} & \frac{\sqrt{3}}{2} \\ -\frac{\sqrt{3}}{2} & -\frac{1}{2} \end{pmatrix}.$$

Equating entries, we obtain a system of four homogeneous linear equations, $M\mathbf{z} \;=\; \mathbf{0}$, for the unknowns

$\mathbf{z} = (a,b,c,d)^\top$. The matrix M has rank three and its null space is spanned by the vector $(1,-i,-i,-1)^\top$. Thus,

$$A^{12} \;=\; b_\star \begin{pmatrix} 1 & -i \\ -i & -1 \end{pmatrix}, \text{where } b_\star \;=\; \langle \partial_{y_1}\Phi_1, \xi\ \partial_{y_1}\Phi_2\rangle \ .$$

Furthermore, since $A^{lj}_{\alpha\beta} \;=\; \overline{A^{jl}_{\beta\alpha}}$, we find:

$$A^{21} \;=\; \overline{b_\star} \begin{pmatrix} 1 & i \\ i & -1 \end{pmatrix} \ .$$

This proves part (2) of Proposition C.3.

Appendix F: $\mathrm{v}_D \geq 0$ and $b_\star \geq 0$; Proof of Proposition A.5

We begin by recalling the expressions for v_D and $b_\star$ in (A13) and (A14):

$$\mathrm{v}_D = \langle \Phi_1, \mathcal{A}_1\Phi_2\rangle, \qquad b_\star \;=\; \langle \partial_{x_1}\Phi_1,\ \xi\ \partial_{x_1}\Phi_2\rangle \ .$$

We will consider two coordinate systems (with coordinates denoted by $\mathbf{x}$ and $\mathbf{x}'$) that differ by a rotation. We define v_D and $b_\star$ as the quantities in the $\mathbf{x}$ coordinate system and v'_D and $b'_\star$ as the quantities in the $\mathbf{x}'$ coordinate system. We will assume that v'_D and $b'_\star$ are complex and then demonstrate that, by rotating the unprimed coordinate system relative to the primed coordinate system (as well as making an appropriate phase choice for the eigenstates), v_D and $b_\star$ can be made to be real.

Introduce a rotation of coordinates from $\mathbf{x} = (x_1, x_2)$ to $\mathbf{x}' = (x'_1, x'_2)$ related by:

$$\mathbf{x}' \;=\; \begin{pmatrix} x'_1 \\ x'_2 \end{pmatrix} \;=\; \begin{pmatrix} \cos\theta & -\sin\theta \\ \sin\theta & \cos\theta \end{pmatrix} \begin{pmatrix} x_1 \\ x_2 \end{pmatrix} \;=\; R_\theta\ \mathbf{x}.$$

We therefore have

$$\begin{aligned} \frac{\partial}{\partial x_1} \;&=\; \frac{\partial x'_1}{\partial x_1}\,\frac{\partial}{\partial x'_1} \;+\; \frac{\partial x'_2}{\partial x_1}\,\frac{\partial}{\partial x'_2} \\ &=\; \cos\theta\ \frac{\partial}{\partial x'_1} \;+\; \sin\theta\ \frac{\partial}{\partial x'_2} \\ &=\; \zeta\cdot\nabla_{\mathbf{x}'}, \quad \zeta = (\cos\theta, \sin\theta). \end{aligned} \tag{F1}$$

Now given any function $f(\mathbf{x})$, we define

$$f'(\mathbf{x}') = \mathcal{R}_\theta[f](\mathbf{x}') \;=\; f\left(R^*_\theta \mathbf{x}'\right),$$

and introduce the rotated Bloch eigenfunctions:

$$\Phi'_j(\mathbf{x}') \;=\; \mathcal{R}_\theta[\Phi_j](\mathbf{x}')\ ,\ j = 1,2.$$

These satisfy the equations for the structure defined by $\xi' = \mathcal{R}_\theta[\xi]$, $\rho' = \mathcal{R}_\theta[\rho]$, and $V' = \mathcal{R}_\theta[V]$:

$$\left[-\nabla_{\mathbf{x}'}\cdot\xi'\ \nabla_{\mathbf{x}'} + V'\right]\Phi'_j \;=\; E_D\ \rho'\ \Phi'_j.$$

Using the notation,

$$\mathcal{A}'_m \;=\; \frac{1}{i}\xi'\partial_{x'_m} \;+\; \frac{1}{i}\partial_{x'_m}(\xi'\ \cdot)$$

and the identities (equation (A11)): $\langle \Phi'_1,\ \mathcal{A}'_1\Phi'_2\rangle \;=\; \mathrm{v}'_D$, $\langle \Phi'_1,\ \mathcal{A}'_2\Phi'_2\rangle = i\mathrm{v}'_D$, we have:

$$\begin{aligned} \mathrm{v}_D \;&\equiv\; \langle \Phi_1,\ \mathcal{A}_1\Phi_2\rangle \\ &=\; \langle \Phi'_1,\ \zeta\cdot\mathcal{A}'\Phi'_2\rangle \\ &=\; \cos\theta\ \langle \Phi'_1,\ \mathcal{A}'_1\Phi'_2\rangle \;+\; \sin\theta\ \langle \Phi'_1,\ \mathcal{A}'_2\Phi'_2\rangle \\ &=\; \mathrm{v}'_D\ e^{i\theta}. \end{aligned} \tag{F2}$$

We now turn to considering $b_\star$ in a rotated coordinate system. Recalling the notation:

$$A^{lj}_{\alpha\beta} \;=\; \left\langle \partial_{y_\alpha}\Phi_l, \xi\ \partial_{y_\beta}\Phi_j\right\rangle, \quad j,l,\alpha,\beta = 1,2\ ,$$

we have

$$\begin{aligned} b_\star \;&=\; \langle \partial_{x_1}\Phi_1,\ \xi\ \partial_{x_1}\Phi_2\rangle \\ &=\; \langle (\zeta\cdot\nabla_{\mathbf{x}'})\Phi'_1,\ \xi'\ (\zeta\cdot\nabla_{\mathbf{x}'})\Phi'_2\rangle \\ &=\; \cos^2\theta\left\langle \partial_{x'_1}\Phi'_1,\ \xi'\ \partial_{x'_1}\Phi'_2\right\rangle \\ &\quad +\ \sin^2\theta\left\langle \partial_{x'_2}\Phi'_1,\ \xi'\ \partial_{x'_2}\Phi'_2\right\rangle + \ \sin\theta\ \cos\theta \\ &\quad \times\Big(\ \left\langle \partial_{x'_2}\Phi'_1,\ \xi'\ \partial_{x'_1}\Phi'_2\right\rangle \;+\; \left\langle \partial_{x'_1}\Phi'_1,\ \xi'\ \partial_{x'_2}\Phi'_2\right\rangle\ \Big) \\ &= \cos^2\theta\ (A')^{12}_{11} \;+\; \sin^2\theta\ (A')^{12}_{22} \\ &\quad +\ \sin\theta\ \cos\theta\left(\ (A')^{12}_{21} + (A')^{12}_{12}\ \right) \end{aligned}$$

The previous expression may be simplified using Proposition C.3, yielding

$$b_\star \;=\; (\cos^2\theta - \sin^2\theta)\ b'_\star \;-2i\sin\theta\cos\theta\ b'_\star \;=\; e^{-2i\theta}\ b'_\star \tag{F3}$$

Explicitly, (F2) and (F3) state:

$$\begin{aligned} \langle \Phi_1,\ \mathcal{A}_1\Phi_2\rangle \;&=\; e^{i\theta}\ \langle \Phi'_1,\ \mathcal{A}'_1\Phi'_2\rangle \\ \langle \partial_{x_1}\Phi_1,\ \xi\ \partial_{x_1}\Phi_2\rangle \;&=\; e^{-2i\theta}\ \left\langle \partial_{x'_1}\Phi'_1,\ \xi'\ \partial_{x'_1}\Phi'_2\right\rangle, \end{aligned} \tag{F4}$$

where θ is to be chosen. Here, $\Phi'_1(\mathbf{x}) \in L^2_{\mathbf{K},\tau}$ and $\Phi'_2(\mathbf{x}) = \overline{\Phi'_1(-\mathbf{x})} \in L^2_{\mathbf{K},\overline{\tau}}$ are any choice of Bloch states in the primed coordinate system.

We next exploit the phase degree of freedom in the choice of these states. In particular, replace Φ'_1 by $e^{i\phi}\Phi'_1 \in L^2_{\mathbf{K},\tau}$ and hence Φ'_2 by $e^{-i\phi}\Phi'_2 \in L^2_{\mathbf{K},\overline{\tau}}$, where now both θ and ϕ are to be determined. Therefore, (F4) becomes

$$\begin{aligned} \mathrm{v}_D \;&\equiv\; \langle \Phi_1,\ \mathcal{A}_1\Phi_2\rangle \\ &=\; e^{i(\theta-2\phi)}\ \langle \Phi'_1,\ \mathcal{A}'_1\Phi'_2\rangle \\ &=\; e^{i(\theta-2\phi)}\ \mathrm{v}'_D \\ b_\star \;&\equiv \langle \partial_{x_1}\Phi_1,\ \xi\ \partial_{x_1}\Phi_2\rangle \\ &=\; e^{-2i(\theta+\phi)}\ \left\langle \partial_{x'_1}\Phi'_1,\ \xi'\ \partial_{x'_1}\Phi'_2\right\rangle \\ &=\; e^{-2i(\theta+\phi)}\ b'_\star\ . \end{aligned} \tag{F5}$$

Hence, if we choose

$$\theta = -\frac{1}{3}\arg \mathrm{v}_D' + \frac{1}{3}\arg b_\star'$$
$$\phi = \frac{1}{3}\arg \mathrm{v}_D' + \frac{1}{6}\arg b_\star'$$

then we obtain $\mathrm{v}_D \geq 0$ and $b_\star \geq 0$. This completes the proof of Proposition A.5.

We now confirm that the effective Hamiltonian transforms as expected under a rotation of coordinates. Let $\mathcal{H}_{\text{eff}}$ and $\mathcal{H}'_{\text{eff}}$ be the effective Hamiltonians written in the $\mathbf{x}$ and $\mathbf{x}'$ coordinate systems, respectively. We choose the $\mathbf{x}$ coordinates so that v_D and $b_\star$ are real (as shown above, this is always possible). As before, we take the two coordinate systems to be related by $\mathbf{x}' = R_\theta \mathbf{x}$ with

$$R_\theta = \begin{pmatrix} \cos\theta & -\sin\theta \\ \sin\theta & \cos\theta \end{pmatrix} \tag{F6}$$

In the primed coordinate system, v_D' and $b_\star'$ are in general complex. Let U and U' be the strain matrices computed in the $\mathbf{x}$ and $\mathbf{x}'$ coordinate systems, respectively, and denote $\mathbf{p} = -i\nabla_{\mathbf{x}}$ and $\mathbf{p}' = -i\nabla_{\mathbf{x}'}$. From Eq. D29 (combined with the convention for the eigenvalue problem in Eq. D5), we have

$$\begin{aligned}
\mathcal{H}'_{\text{eff}} &= \begin{pmatrix} 0 & \overline{\mathrm{v}_D'}\,(p_1' - ip_2') \\ \mathrm{v}_D'\,(p_1' + ip_2') & 0 \end{pmatrix} \\
&- 2\begin{pmatrix} 0 & \overline{b_\star'}\big(\mathrm{tr}(\sigma_3 U') + i\,\mathrm{tr}(\sigma_1 U')\big) \\ b_\star'\big(\mathrm{tr}(\sigma_3 U') - i\,\mathrm{tr}(\sigma_1 U')\big) & 0 \end{pmatrix} \\
&- 2a_\star' \mathrm{tr}(U'\sigma_0)\begin{pmatrix} 1 & 0 \\ 0 & 1 \end{pmatrix}.
\end{aligned} \tag{F7}$$

The effective Hamiltonian in the unprimed coordinates is given by Eq. D5

$$\mathcal{H}_{\text{eff}} \;=\; \mathrm{v}_D\,(\mathbf{p} - \mathbf{A}_{\text{eff}})\cdot\sigma \;+\; W_{\text{eff}}\;\sigma_0 \tag{F8}$$

with

$$\begin{aligned}
W_{\text{eff}} &= -2a_\star\;\mathrm{tr}\,(U\sigma_0) \\
\mathbf{A}_{\text{eff}} &= \frac{2b_\star}{\mathrm{v}_D}\begin{pmatrix} +\mathrm{tr}\,(U\sigma_3) \\ -\mathrm{tr}\,(U\sigma_1) \end{pmatrix}.
\end{aligned} \tag{F9}$$

As discussed above, we have

$$\mathrm{v}_D' = \mathrm{v}_D e^{-i\theta} \qquad b_\star' = b_\star e^{2i\theta} \tag{F10}$$

We now simplify each of the three terms in Eq. F7. Using Eq. F10 gives for the first term:

$$\begin{aligned}
&\begin{pmatrix} 0 & \overline{\mathrm{v}_D'}\,(p_1' - ip_2') \\ \mathrm{v}_D'\,(p_1' + ip_2') & 0 \end{pmatrix} \\
&= \mathrm{v}_D\Big(p_1'(\cos\theta\,\sigma_1 - \sin\theta\,\sigma_2) + p_2'(\sin\theta\,\sigma_1 + \cos\theta\,\sigma_2)\Big) \\
&= \mathrm{v}_D\,\mathbf{p}'\cdot\sigma'
\end{aligned} \tag{F11}$$

where in the last line we have defined rotated Pauli matrices $\sigma_j' = \mathcal{V}\sigma_j\mathcal{V}^*$ with $\mathcal{V} = e^{i\theta(\sigma_3/2)}$. Equivalently, the rotated Pauli matrices are given by:

$$\begin{pmatrix} \sigma_1' \\ \sigma_2' \end{pmatrix} = \begin{pmatrix} \cos\theta & -\sin\theta \\ \sin\theta & \cos\theta \end{pmatrix}\begin{pmatrix} \sigma_1 \\ \sigma_2 \end{pmatrix}. \tag{F12}$$

Using Eq. F10, we have for the second term of Eq. F7

$$\begin{aligned}
&\begin{pmatrix} 0 & -2\overline{b_\star'}\big(\mathrm{tr}(\sigma_3 U') + i\,\mathrm{tr}(\sigma_1 U')\big) \\ -2b_\star'\big(\mathrm{tr}(\sigma_3 U') - i\,\mathrm{tr}(\sigma_1 U')\big) & 0 \end{pmatrix} \\
&= -2b_\star\Big(\big[\,\mathrm{tr}(\sigma_3 U')\cos 2\theta + \mathrm{tr}(\sigma_1 U')\sin 2\theta\,\big]\sigma_1 \\
&\qquad + \big[\,\mathrm{tr}(\sigma_3 U')\sin 2\theta - \mathrm{tr}(\sigma_1 U')\cos 2\theta\,\big]\sigma_2\Big) \\
&= -2b_\star\Big(\big[\,\mathrm{tr}(\sigma_3 U')\cos 3\theta + \mathrm{tr}(\sigma_1 U')\sin 3\theta\,\big]\sigma_1' \\
&\qquad + \big[\,\mathrm{tr}(\sigma_3 U')\sin 3\theta - \mathrm{tr}(\sigma_1 U')\cos 3\theta\,\big]\sigma_2'\Big) \\
&= -\mathrm{v}_D\,\mathbf{A}_{\text{eff}}'\cdot\sigma'
\end{aligned} \tag{F13}$$

where we have defined

$$\mathbf{A}_{\text{eff}}' = \frac{2b_\star}{\mathrm{v}_D}\begin{pmatrix} \cos 3\theta & -\sin 3\theta \\ \sin 3\theta & \cos 3\theta \end{pmatrix}\begin{pmatrix} +\mathrm{tr}(\sigma_3 U') \\ -\mathrm{tr}(\sigma_1 U') \end{pmatrix}. \tag{F14}$$

To relate $\mathbf{A}_{\text{eff}}'$ to $\mathbf{A}_{\text{eff}}$, we note that $U' = R_\theta U R_\theta^T$. Hence, Eq. F14 becomes

$$\begin{aligned}
\mathbf{A}_{\text{eff}}' &= \frac{2b_\star}{\mathrm{v}_D}\begin{pmatrix} \cos 3\theta & -\sin 3\theta \\ \sin 3\theta & \cos 3\theta \end{pmatrix}\begin{pmatrix} +\mathrm{tr}(R_\theta^T\sigma_3 R_\theta U) \\ -\mathrm{tr}(R_\theta^T\sigma_1 R_\theta U) \end{pmatrix} \\
&= \frac{2b_\star}{\mathrm{v}_D}\begin{pmatrix} \cos 3\theta & -\sin 3\theta \\ \sin 3\theta & \cos 3\theta \end{pmatrix}\begin{pmatrix} \cos 2\theta & \sin 2\theta \\ -\sin 2\theta & \cos 2\theta \end{pmatrix} \\
&\qquad \times \begin{pmatrix} +\mathrm{tr}(\sigma_3 U) \\ -\mathrm{tr}(\sigma_1 U) \end{pmatrix} \\
&= \frac{2b_\star}{\mathrm{v}_D}\begin{pmatrix} \cos\theta & -\sin\theta \\ \sin\theta & \cos\theta \end{pmatrix}\begin{pmatrix} +\mathrm{tr}(\sigma_3 U) \\ -\mathrm{tr}(\sigma_1 U) \end{pmatrix} \\
&= R_\theta\,\mathbf{A}_{\text{eff}}.
\end{aligned} \tag{F15}$$

Note also that $\mathbf{p}' = R_\theta\mathbf{p}$. Finally, from the expression for $a_\star$ in Theorem D.1, it is clear that $a_\star' = a_\star$. Hence, for the third term in Eq. F7, we have

$$\begin{aligned}
W_{\text{eff}}' \equiv -2a_\star'\mathrm{tr}(U'\sigma_0) &= -2a_\star\mathrm{tr}(UR_\theta^T\sigma_0 R_\theta) \\
&= W_{\text{eff}}.
\end{aligned} \tag{F16}$$

Putting all of this together, we have

$$\begin{aligned}
\mathcal{H}_{\text{eff}} &\;=\; \mathrm{v}_D\,(\mathbf{p} \;-\mathbf{A}_{\text{eff}})\cdot\sigma \;\;+\; W_{\text{eff}}\;\sigma_0 \\
\mathcal{H}'_{\text{eff}} &\;=\; \mathrm{v}_D\,(\mathbf{p}' - \mathbf{A}'_{\text{eff}})\cdot\sigma' \;+\; W'_{\text{eff}}\;\sigma'_0
\end{aligned} \tag{F17}$$

where

$$\begin{aligned}
&\mathbf{A}'_{\text{eff}} = R_\theta\mathbf{A}_{\text{eff}} && \mathbf{p}' = R_\theta\mathbf{p} \\
&W'_{\text{eff}} = W_{\text{eff}} && \sigma_j' = \mathcal{V}\sigma_j\mathcal{V}^*
\end{aligned}$$

with $\mathcal{V} = e^{i\theta(\sigma_3/2)}$.

[1] C. L. Kane and E. J. Mele, Phys. Rev. Lett. **78**, 1932 (1997).
[2] F. Guinea, M. I. Katsnelson, and A. K. Geim, Nature Physics **6**, 30 (2009).
[3] N. Levy, S. A. Burke, K. L. Meaker, M. Panlasigui, A. Zettl, F. Guinea, A. H. C. Neto, and M. F. Crommie, Science **329**, 544 (2010).
[4] K. Gomes, W. Mar, W. Ko, F. Guinea, and H. Manoharan, Nature **483** (2012).
[5] J. L. Mañes, F. de Juan, M. Sturla, and M. A. H. Vozmediano, Phys. Rev. B **88**, 155405 (2013).
[6] B. Amorim, A. Cortijo, F. de Juan, A. Grushin, F. Guinea, A. Gutiérrez-Rubio, H. Ochoa, V. Parente, R. Roldán, P. San-Jose, J. Schiefele, M. Sturla, and M. Vozmediano, Physics Reports **617**, 1 (2016).
[7] R. O. Umucalılar and I. Carusotto, Phys. Rev. A **84**, 043804 (2011).
[8] M. Hafezi, E. A. Demler, M. D. Lukin, and J. M. Taylor, Nature Physics **7**, 907 (2011).
[9] K. Fang, Z. Yu, and S. Fan, Nature Photonics **6**, 782 (2012).
[10] K. Fang, J. Luo, A. Metelmann, M. H. Matheny, F. Marquardt, A. A. Clerk, and O. Painter, Nature Physics **13**, 465 (2017).
[11] E. M. Purcell, Phys. Rev. **69**, 681 (1946).
[12] T. F. Krauss, Nature Photonics **2**, 448 (2008).
[13] M. C. Rechtsman, J. M. Zeuner, A. Tünnermann, S. Nolte, M. Segev, and A. Szameit, Nature Photonics **7**, 153 (2012).
[14] O. Jamadi, E. Rozas, G. Salerno, M. Milićević, T. Ozawa, I. Sagnes, A. Lemaître, L. L. Gratiet, A. Harouri, I. Carusotto, J. Bloch, and A. Amo, "Direct observation of photonic Landau levels and helical edge states in strained honeycomb lattices," (2020), arXiv:2001.10395 [cond-mat.mes-hall].
[15] G. Salerno, T. Ozawa, H. M. Price, and I. Carusotto, 2D Materials **2**, 034015 (2015).
[16] M. Bellec, C. Poli, U. Kuhl, F. Mortessagne, and H. Schomerus, "Observation of supersymmetric pseudo-Landau levels in strained microwave graphene," (2020), arXiv:2001.10287 [cond-mat.mes-hall].
[17] H. Schomerus and N. Y. Halpern, Phys. Rev. Lett. **110**, 013903 (2013).
[18] C. Brendel, V. Peano, O. J. Painter, and F. Marquardt, Proceedings of the National Academy of Sciences (2017), 10.1073/pnas.1615503114.
[19] H. Abbaszadeh, A. Souslov, J. Paulose, H. Schomerus, and V. Vitelli, Phys. Rev. Lett. **119**, 195502 (2017).
[20] X. Wen, C. Qiu, Y. Qi, L. Ye, M. Ke, F. Zhang, and Z. Liu, Nature Physics **15**, 352 (2019).
[21] J. Joannopoulos, S. Johnson, J. Winn, and R. Meade, *Photonic Crystals: Molding the Flow of Light* (Princeton University Press, 2011).
[22] C. L. Fefferman and M. I. Weinstein, Journal of the American Mathematical Society **25**, 1169 (2012).
[23] C. L. Fefferman and M. I. Weinstein, Communications in Mathematical Physics **326**, 251 (2014).
[24] J. P. Lee-Thorp, M. I. Weinstein, and Y. Zhu, Archive for Rational Mechanics and Analysis **232**, 1 (2019).
[25] S. Barik, H. Miyake, W. DeGottardi, E. Waks, and M. Hafezi, New Journal of Physics **18**, 113013 (2016).
[26] C. L. Fefferman, J. P. Lee-Thorp, and M. I. Weinstein, Annals of PDE **2** (2016).
[27] A. Drouot and M. Weinstein, Advances in Mathematics **368**, 107142 (2020).
[28] S. G. Johnson and J. D. Joannopoulos, Opt. Express **8**, 173 (2001).
[29] D. Melati, A. Melloni, and F. Morichetti, Adv. Opt. Photon. **6**, 156 (2014).
[30] C. L. Fefferman and M. I. Weinstein, J. Amer. Math. Soc. **25**, 1169 (2012).
[31] C. L. Fefferman and M. I. Weinstein, Commun. Math. Phys. **326**, 251 (2014).
[32] J. P. Lee-Thorp, M. I. Weinstein, and Y. Zhu, Arch. Rational Mech. Anal. **232**, 1 (2019).
[33] L. D. Landau and E. M. Lifshitz, *Quantum Mechanics: Non-relativistic Theory* (Pergamon Press, 1977).